British Geological Survey

NATURAL ENVIRONMENT RESEARCH COUNCIL

A REVISION OF *REDUVIASPORONITES* WILSON 1962: DESCRIPTION, ILLUSTRATION, COMPARISON AND BIOLOGICAL AFFINITIES

Internal Report IR/02/005

BRITISH GEOLOGICAL SURVEY

INTERNAL REPORT IR/02/005

A REVISION OF REDUVIASPORONITES WILSON 1962: DESCRIPTION, ILLUSTRATION, COMPARISON AND BIOLOGICAL AFFINITIES

FOSTER, C. B , STEPHENSON, M . H., MARSHALL, C., LOGAN, G. A., and GREENWOOD, P.

Key words

Palynology Permian Triassic.

Bibliographical reference

FOSTER, C. B , STEPHENSON, M . H., MARSHALL, C., LOGAN, G. A., AND GREENWOOD, P. 2001. A REVISION OF REDUVIASPORONITES WILSON 1962: DESCRIPTION, ILLUSTRATION, COMPARISON AND BIOLOGICAL AFFINITIES. *British Geological Survey Internal Report*, IR/02/005. 29pp.

Keyworth, Nottingham British Geological Survey 2001

BRITISH GEOLOGICAL SURVEY

The full range of Survey publications is available from the BGS Sales Desks at Nottingham and Edinburgh; see contact details below or shop online at www.thebgs.co.uk

The London Information Office maintains a reference collection of BGS publications including maps for consultation.

The Survey publishes an annual catalogue of its maps and other publications; this catalogue is available from any of the BGS Sales Desks.

The British Geological Survey carries out the geological survey of Great Britain and Northern Ireland (the latter as an agency service for the government of Northern Ireland), and of the surrounding continental shelf, as well as its basic research projects. It also undertakes programmes of British technical aid in geology in developing countries as arranged by the Department for International Development and other agencies.

The British Geological Survey is a component body of the Natural Environment Research Council.

Keyworth, Nottingham NG12 5GG

✍ 0115-936 3241 Fax 0115-936 3488
e-mail: sales@bgs.ac.uk
www.bgs.ac.uk
Shop online at: www.thebgs.co.uk

Murchison House, West Mains Road, Edinburgh EH9 3LA

✍ 0131-667 1000 Fax 0131-668 2683
e-mail: scotsales@bgs.ac.uk

London Information Office at the Natural History Museum (Earth Galleries), Exhibition Road, South Kensington, London SW7 2DE

✍ 020-7589 4090 Fax 020-7584 8270
✍ 020-7942 5344/45 email: bgslondon@bgs.ac.uk

Forde House, Park Five Business Centre, Harrier Way, Sowton, Exeter, Devon EX2 7HU

✍ 01392-445271 Fax 01392-445371

Geological Survey of Northern Ireland, 20 College Gardens, Belfast BT9 6BS

✍ 028-9066 6595 Fax 028-9066 2835

Maclean Building, Crowmarsh Gifford, Wallingford, Oxfordshire OX10 8BB

✍ 01491-838800 Fax 01491-692345

Parent Body

Natural Environment Research Council, Polaris House, North Star Avenue, Swindon, Wiltshire SN2 1EU

✍ 01793-411500 Fax 01793-411501
www.nerc.ac.uk

1 Acknowledgements

This paper relies heavily on access to rock samples and palynological strew slides containing *R. chalastus* from many different parts of the globe. For this generous exchange of material we are grateful to: B. E Balme, and R. Helby (Australia), H. Wopfner (Germany), O. P. Yaroshenko (Russia), H. Visscher (Netherlands), G. Warrington (UK), and the late L. R. Wilson (USA). Russian material was collected by CBF under the DIST-funded Australia-Russia exchange scheme: Chinese samples were collected by CBF as part of an ARC funded research project Grant No. A39906543 awarded to Ian Metcalfe. For geochemical analyses of *R. chalastus* and discussion we are grateful to R. E Summons and C. Boreham (Geoscience Australia). Foster publishes with the permission of the CEO of Geoscience Australia. Stephenson publishes with the permission of the Executive Director, British Geological Survey. The Saudi Arabian Oil Company (Saudi Aramco) kindly gave its permission to use a sample from the DILM-1 well for this study.

Contents

Summary

Optical and electron microscopy of topotype material confirms that *Reduviasporonites* Wilson 1962 is the senior synonym of *Chordecystia* Foster 1979, and *Tympanicysta* Balme 1980. Moreover the type species of the last two genera, assigned in 1999 to *Reduviasporonites* by Elsik as *R. chalastus* (Foster) and *R. stochianus* (Balme), are conspecific. The type species, *R. catenulatus* Wilson 1962, differs from *R. chalastus* in that its constituent cells are significantly smaller, more rounded, and have less well developed connecting areas (terminal rims) between cells. *Brazilea helbyi* forma *gregata* Foster 1979, recorded only from the type material of *R. chalastus*, is likely to be a junior synonym of that taxon.

The stratigraphical occurences of the species of *Reduviasporonites* suggest that *R. catenulatus* is most common in the Wordian (Kazanian) of Oklahoma, though specimens of the size range associated with *R. catenulatus* are present very rarely in the Early Triassic Mazzin Member of the Werfen Formation, Austria. *R. chalastus* is present in Changhsingian to Griesbachian rocks spanning several million years and is therefore present outside narrow sequences spanning the Permian-Triassic boundary. The size of the constituent cells present in *R. chalastus* appears to be

related to palaeolatitude with large examples occurring in the palaeotemperate Permian of China, Russia, and Australia (Moura) and smaller specimens occurring in the palaeotropical and paleoequatorial Permian of northern Australia, Saudi Arabia, UK and Austria.

Geochemical analysis of *R. chalastus* from the Mazzin Member (Lower Triassic, Austria) suggests that it may be of algal rather than fungal origin. This implies that *R. chalastus* is unlikely to be integral to the process of mass extinction occurring at or near the Permian-Triassic boundary, as suggested by Visscher and other workers, because it appears to range outside the postulated time of mass extinction, and because as a probable alga rather than a fungus, it cannot have acted as a saprophytic metaboliser of dead vegetation formed in the extinction event.

2 Introduction

A 'spike' of supposed fungal spores occurs at the Permian-Triassic boundary in various locations, in close association with a mass extinction event (Erwin 1993). This close relationship has lead palynologists (Eshet et al., 1995; Visscher et al., 1996; Elsik, 1999) to consider that the supposed fungus may have been a saprophytic metaboliser of dead vegetation formed during the extinction event. Elsik (1999) suggested that two of the taxa often associated with the 'fungal spike': *Chordecystia* Foster 1979 from the Australian Rewan Formation, and *Tympanicysta* Balme 1980 from the Martinia Shale, Greenland, are junior synonyms of *Reduviasporonites* Wilson 1962, and affirmed a fungal origin for the latter. It is not clear if topotype material was reexamined to support this conclusion. In contrast Krassilov et al. (1999) suggested that 'spores' assigned by Russian palynologists to *Tympanicysta* are more closely allied to the zygnemataceaen algae.

For this study, we have examined topotype material of *Reduviasporonites catenulatus* Wilson 1962 and *Reduviasporonites chalastus* (Foster) Elsik 1999, including its junior synonym *Tympanicysta stoschiana*, as well as well-preserved specimens of these taxa from Greenland, Britain, China, Saudi Arabia, Russia, Australia and Austria, to allow comparative study. Details of the samples are given in Appendix 1.

The aims of the project are to determine whether:

- the taxa are synonymous;
- the taxa have fungal or algal origins.

3 Systematic palaeontology

3.1 DEFINITION OF TERMS

The origin of the forms described in this paper is uncertain; they have been described as being of fungal origin (Wood and Elsik, 1999; Elsik, 1999; Visscher et al., 1996) and of possible algal origin (Krassilov et al., 1999). In view of this uncertainty a new terminology independent of mycology and phycology is adopted. New terms suggested are (see Text-Figure 1):

Cell: the main unit of chains; usually hollow and cylindrical, but may be Y-shaped, ovoid or spherical.

Terminal rim: the, darkened, slightly protuberant annular thickening usually present at the termini or opposite margins of the cell.

Terminal plane: the usually circular or rectangular area enclosed by the terminal rim, which is perpendicular in orientation to the long axis of the cell.

Inner body: the thin walled body, internal to the cell, that normally mimics the overall shape of the cell but which may be of various shapes depending on the extent of its shrinkage.

3.2 TAXONOMY

Genus *Reduviasporonites* Wilson 1962 emend.

1962 *Reduviasporonites* Wilson: p. 91-93; pl. 1, figs. 1-6

1979 *Chordecystia* Foster: p. 109-110; pl 41, figs. 3-9; text-fig. 22

1980 *Tympanicysta* Balme: p. 22-24; pl. 1, figs. 3-7

Type species by original designation: *R. catenulatus* Wilson 1962

Emended generic diagnosis

Microfossil, usually forming chains, but also present as pairs of cells or single dispersed cells. Cell outline usually subcircular or subrectangular, though more rarely can be flask-, spindle- or 'Y' shaped. Most cells contain an inner body of the same shape as the outer cell that may be adpressed to the inner surface of the main cell so that it is difficult to distinguish optically. The inner body may also occupy a smaller part of the cell cavity (?through shrinkage). Outer cell wall approximately 0.5-1µm thick, though may be locally thicker; smooth; inner body wall less than 1 µm thick, smooth. Cells in chains are joined by thickened parts of the outer cell wall; these may be regular rim – like structures or simple irregular thickenings. Cells may have up to three of these thickenings allowing branched chains to form.

Generic description

Cell shape (see Text-Figure 2): The two known species of Reduviasporonites can be distinguished partly by cell shape but this can also vary considerably within a single assemblage of one or other taxon. R. catenulatus is always subcircular or oval in outline, suggesting an original, uncompressed spherical or ovoid shape. In R. chalastus, the most common outline by far is subrectangular and this is consistent with SEM evidence suggesting that most cells of these taxa were originally cylindrical in shape with a length:width ratio of between 1:1 and 4:1. Also occurring in assemblages of R. chalastus are flask shaped, ovoid and spherical cells. In the British and Saudi Arabian assemblages of R. chalastus, rare spindle shaped specimens with constricted and protuberant terminal rims (Plate 2, Fig. 17; Plate 5, Fig. 6) occur. Very rare are 'three way cells' which have three terminal rims; these commonly have a 'Y' shape (Plate 3, Fig. 4; Plate 4, Fig. 14; Plate 5, Figs. 10, 14).

Outer cell wall: The outer cell wall of Reduviasporonites is between 0.5 and 1.5? m thick. When well preserved the outer surface of the cell wall is smooth or very finely and regularly granulate; but when poorly preserved the surface is irregularly punctate or intragranulate. The outer cell

wall seems particularly susceptible to pyritisation and commonly displays a surface irregularly pitted with the rectangular marks of invasive pyrite growth. The colour of the outer cell wall is often darker than other palynomorphs in the same assemblage, and may contain more natural pigment than associated spores and pollen.

Many specimens show 'striations' in the outer wall of the cell, usually orientated parallel to the long axis of the cell (Plate 2, Figs. 2-3, 6), and in rare cases perpendicular to it. These may be due to shrinkage related to dessication, and are most common in narrow cells or cells with constricted and protuberant terminal rims.

Inner body: An inner body has been observed in most specimens of R. chalastus though not as yet in R. catenulatus. In the former, the inner cell wall is usually less than 0.5 ?m thick and its surface is smooth in the few specimens where it is exposed. The inner body commonly has the same shape as the outer cell and may be adpressed to the inner surface of the main cell so that it is difficult to distinguish optically. Through shrinkage, it may occupy a smaller part of the cell cavity and may be twisted. Shrinkage first occurs in the middle parts; usually the termini of the inner body are firmly attached to the inner surface of the terminal rim. With further shrinkage these finally detach from the outer cell wall. Text-Figure 3 illustrates possible stages of shrinkage.

Cell material: Dark cell material has been observed in most specimens of R. chalastus though not as yet in R. catenulatus. In the former, this is present is most cells and appears to occur within the inner body. The material was recorded by Balme (1980) as 'amorphous material'; the present study confirms it is, in many cases, structureless, but in the best preserved specimens (Plate 1, Figs. 4-7; Plate 4, Fig. 1, 3) appears dark, dense and granulate. In a number of specimens the material is clearly seen to be enveloped by the delicate, shrunken inner body (Plate 2, Fig. 11; Plate 3, Figs. 11-12;). Krassilov et al. (1999) who considered Tympanicysta to be of algal origin, suggested that the cell material corresponds to the 'chloroplast of zygnematalean algae…'.

Folding patterns (see Text-Figures 4 and 5): Thinner walled specimens of R. chalastus have a characteristic diagonal folding pattern (Text-Figure 4). Observation and modeling of the cell by the authors suggests that this is caused by twisting of the cell body about the long axis of the cell. Other folds, in either of the cell walls, commonly delineate rectilinear shapes and these may represent areas of residual attachment of the inner and outer cell walls. Commonly short lunate folds, orientated perpendicular to the long axis of the cell, occur close to the margins of ovoid cells (Text-Figure 4). These are believed to result from the attachment of the termini of the inner body to the inner surface of the outer body and as such may represent parts of a poorly developed terminal rim.

Within the cell wall of *R. catenulatus,* folding patterns are rather random in chains of cells, or occasionally subcircular and concentric in arrangement in the case of single cells (Text-Figure 5; Plate 6, Figs. 5, 7, 8, 9, 33, 36).

Terminal rim: The terminal rim is an annular thickening or fold, occurring at the cell terminus, which appears to allow the cells to connect into chains. This rim is usually well-developed in R. chalastus but very rare in R. catenulatus. The rim is firmly attached on its inner surface to the termini of the inner body. Close to the base of the terminal rim is an incipient weakness in the outer cell wall which allows it to be partially or wholly detached from the rest of the cell (Plate 3, Figs. 5, 14). The terminal rim is often discontinuous (Plate 1 Fig. 3; Plate 2, Figs. 13, 15). Light microscopy indicates that the few specimens that display 'end on' views of the terminal face have no aperture (Plate 1, Fig. 12; Plate 3, Fig. 7) but SEM images (e.g. Plate 5, Fig. 13)

suggest that other specimens have an indistinct, raised boss-like feature in the centre of the terminal rim.

Chain formation: Chains of cells were observed in all the assemblages studied, some reaching up to 15 cells long. Occasionally the three terminal rims of 'Y' shaped cells allow several chains to develop from one cell. Chains in R. catenulatus are less regular in appearance than those of R. chalastus and the means by which cells join is less clear in the former (Text-Figure 6).

Effects of processing on size of cells

In order to investigate the effects of palynological processing techniques on the size of cells, two aliquots of post HF residue from the DILM-1 well, Saudi Arabia, containing abundant *R. chalastus*, were subjected to different oxidation and KOH treatments. The results of these were compared with an untreated post HF residue from the same sample to determine whether size changes had occurred. The treatments were:

1. Aliquot 1 , concentrated Nitric Acid for 1 minute then treatment with 5% KOH;
2. Aliquot 2, concentrated Nitric Acid for 30 minutes then treatment with 10% KOH

The treatments caused no obvious change in cell size or shape and so it was concluded that processing method cannot be responsible for size variability from sample to sample.

Reduviasporonites catenulatus Wilson 1962

Plate 6, figs. 1-36

1962 *Reduviasporonites catenulatus* Wilson: p. 94-95; pl. 1, figs. 1-6

1967 *Reduviasporonites catenulatus* Wilson 1962 – Morgan: pl. 1, fig. 1

Description

Microfossil, usually forming chains, but also present as pairs of cells or single dispersed cells. Cell outline subcircular or subrectangular in outline; probably originally sub-spherical before compression. Outer cell wall approximately 1 µm thick, smooth; may be irregularly thickened at the margins; no inner body or cell material has been observed. Cells in a chain, and particularly single unattached cells, have regular concentric or subpolygonal fold patterns. Method of cell-to-cell attachment not known, though some chains appear to indicate that the convexity of part of a given cell fits into a corresponding hemispherical concavity in an adjacent cell. No terminal rims are present.

Dimensions

(No. of specimens measured 70) Mean length 14.0µm; mean width 14.7µm; standard deviation of lengths 2.4; standard deviation of widths 1.9; maximum length 22µm; maximum width 22µm; minimum length 9µm; minimum width 11µm; mean length to width ratio 0.96.

Reduviasporonites chalastus (Foster) Elsik 1999

Plates 1-5

1979 *Chordecystia chalasta* Foster: p. 109-110; pl 41, figs. 3-9; text-fig. 22

?1979 *Brazilea helbyi* forma *gregata* Foster: p. 112; pl. 41, figs. 1-2

1980 *Tympanicysta stoschiana* Balme: p. 22-24; pl. 1, figs. 3-7

1999 *Reduviasporonites stoschianus* (Balme) Elsik: p. 40; pl. 1, figs. 1-24

Description

Microfossil, usually forming chains but also present as pairs of cells or single dispersed cells. Cell outline subrectangular, rarely oval, irregular or 'Y' shaped, though most cells were probably originally cylindrical in shape before compression. Outer cell wall approximately 0.5µm to 1.5µm thick, smooth, may be slightly thickened in the regions of the terminal rims. The inner body commonly has the same shape as the outer cell and may be adpressed to the inner surface of the main cell so that it is difficult to distinguish optically. The inner body may also occupy a smaller part of the cell cavity (?through shrinkage) and may be twisted. Detachment of the two walls appears first to occur in the middle parts; usually the termini of the inner body are firmly attached to the inner surface of the terminal rim, though detachment at these points may also occur. Wall of inner body 0.5 to 1µm thick where observed, smooth, sometimes hyaline in appearance. Dark 'cell material' of amorphous or granulate appearance occurs in many specimens and is often enveloped by the delicate, shrunken inner body. Cell has a number of characteristic folding patterns. The diagonal folding pattern noted by Foster (1979) is caused by twisting of the cell body about the long axis of the cell. Other folds, in either of the cell walls, commonly delineate rectilinear shapes and these may represent areas of residual attachment of the inner and outer cell walls. Commonly, short lunate folds, orientated perpendicular to the long axis of the cell, occur close to the margins of ovoid cells (see Text-Figure 5). These are believed to result from the attachment of the termini of the inner body to the inner surface of the outer body and as such may represent parts of a poorly developed terminal rim.

Dimensions

(No. of specimens measured 230) Mean length 79.4µm; mean width 38.6µm; standard deviation of lengths 43.2; standard deviation of widths 23.1; maximum length 220µm; maximum width 127µm; minimum length 18µm; minimum width 9µm; mean length to width ratio 2.2.

The lengths and widths of 300 specimens of *R. catenulatus*, and *R. chalastus* are shown on a scattergram (Text-Figure 7) that also delineates the size fields of *R. chalastus* and *R. catenulatus*.

Comparison

R. chalastus is distinguished from *R. catenulatus* by the greater size of its cells (up to 10 times greater in most cases, Text-Figure 7), by the generally rectangular outline shape of its cells, by the presence in its cells of distinct inner bodies, often containing cell material, and by the presence of terminal rims allowing regular articulation of cells into chains. As noted by Elsik (1999) rare, small specimens of *R. chalastus* from the Mazzin Member are similar in size to R. catenulatus (Text-Figure 7) but these have the terminal rims, cell material and distinct inner bodies associated with *R. chalastus*.

Remarks

Our examination of topotype specimens of the Greenland material originally described as *Tympanicysta stoschiana* by Balme (1980) and topotype specimens of Australian material described by Foster (1979) as *Chordecystia chalasta*, shows that they are synonymous. Careful examination of specimens of *Brazilea helbyi* forma *gregata* Foster 1979 suggest that this is also likely to be either synonymous with *R. chalastus*, or a new species of *Reduviasporonites*. Further work on better-preserved material is required to confirm this.

3.3 MORPHOLOGICAL VARIATION IN *R. CHALASTUS*

Variation in size, shape and preservation is evident within and between assemblages of *R. chalastus*. In this section these variations are described in detail.

3.3.1 Junggar, China

The five assemblages from the Junggar section, China (see Appendix 1) contain large numbers of cells in a variety of forms. Elongate, cylindrical cells are common, but ovoid, spherical, 'Y' shaped and flask shaped cells also occur (Plate 3, Figs. 1, 4, 8-10, 15). Overall the cells are rather poorly preserved but this has rendered the outer cell wall relatively transparent so that the inner body and cell material can be examined and photographed (Plate 3, Figs. 2-3). A number of specimens illustrate the shrinkage of the inner body and its twisted appearance (Plate 3, Figs. 2, 11-12). In a few specimens the twisted, shrunken inner body is shown to envelope the cell material (e.g. Plate 3, Figs. 11-12). Other specimens illustrate the incipient weakness in the outer cell wall which occurs at the base of the terminal rim, so that partial (Plate 3, Fig. 14), and full (Plate 3, Fig. 7) detachment of the terminal rim can occur. In terms of range of shapes, preservational condition and size, the Chinese assemblages are most similar to those of Australia (Moura), Russia and Greenland.

3.3.2 Russian Platform

The assemblage from the Russian Platform, Vologodskaya Region (see Appendix 1) contains common elongate, cylindrical cells, but also ovoid and flask-shaped cells (Plate 4, Figs. 1, 3-4) Although relatively well preserved, the outer cell walls are generally relatively transparent, revealing the usually shrunken and twisted inner body, almost always attached to the inner surface of the terminal rim (Plate 4, Figs. 2, 4). A number of cells have poorly developed, discontinuous terminal rims (Plate 4, Fig. 3).

3.3.3 Moura, Bowen Basin, Australia

The two assemblages from the Moura Borehole (Queensland, Australia) (see Appendix 1) contained poorly preserved cells ranging in shape from very regularly cylindrical to ovoid and spherical. Perhaps reflecting this poor preservation, very few cells in chains were noted. A number of cells display the diagonal folds thought by Foster (1979) to be characteristic of *R.*

chalastus (e.g. Plate 1, Fig. 11). A few specimens (e.g. Plate 1, Fig. 12) display 'end on' views of the terminal face which indicate that, in these specimens at least, no aperture is present.

Perhaps due to poor preservation, none of the Moura specimens display the inner body with clarity. In most cases only folds in the inner body are visible due to the increased opacity that this produces. In other specimens, folds in the outer wall of the cell caused by residual attachment of the inner body are visible. Overall these fold patterns suggest that partially shrunken inner bodies are present, usually attached to the inner surface of the terminal rim.

A number of spherical to ovoid cells with folding patterns suggesting cylindrical inner bodies (Plate 1, Figs. 10, 16-17, 18), are closely similar to specimens figured by Foster (1979; pl. 41, figs. 1-2) and assigned by him to *Brazilea helbyi* forma *gregata* Foster 1979.

3.3.4 Kap Stosch, Greenland

The assemblages from Kap Stosch, Greenland (see Appendix 1) contain common elongate, cylindrical cells, but also ovoid and flask shaped cells (Plate 2, Figs. 7-8, 9). Although relatively well preserved, the outer cell walls are generally relatively transparent, revealing the usually shrunken and twisted inner body, almost always attached to the inner surface of the terminal rim (Plate 2, Figs. 3-4).

3.3.5 Billawock, Bonaparte Basin, Australia

The one assemblage and 6 single grain mounts from BHPP Billawock No. 1 borehole, Australia (see Appendix 1) contained well preserved cells ranging in shape from very regularly cylindrical to ovoid (Plate 1, Figs. 1-3). Although the outer cell wall is relatively well preserved and therefore less transparent than in specimens from Moura, the inner bodies are nevertheless revealed in a few specimens (Plate 1, Fig. 1) and granular cell material is very distinct (Plate 1, Figs. 4-7). A number of specimens have poorly developed and discontinuous terminal rims (Plate 1, Fig. 2).

3.3.6 Conisborough, UK

The assemblage from Conisborough contains very well preserved, relatively small (Text-Figure 7) cells ranging in shape from cylindrical, to flask-shaped, spindle-shaped and ovoid. There are more flask and spindle shaped cells than in other assemblages studied (Plate 2, Figs. 16-18). As with the Austrian and Saudi Arabian specimens, the outer cell and inner body have relatively thick walls and the inner bodies, when visible, are almost completely adpressed to the inner cell wall. A number of specimens display longitudinal 'striations' possibly caused by shrinkage (e.g. Plate 2, Fig. 18).

A few specimens (e.g. Plate 2, Fig. 17) display both inner and outer layers and these suggest that the inner body wall is smooth and approximately 1 ?m thick, which is considerably thicker than that seen in Russian, Chinese and Billawock specimens. The outer cell wall in the Conisborough specimens is usually smooth, though a few have a very regular, very small granulate ornament (grana just resolvable using oil x100 objective). Like the inner body wall, the outer cell wall in the Conisborough specimens is relatively thick.

3.3.7 Hilton Plant Beds, UK

The assemblage from the Hilton Plant Beds contains well preserved, relatively small (Text-Figure 7), mainly ovoid cells. Many of the cells have rather poorly developed terminal rims.

3.3.8 DILM-1, Saudi Arabia

The assemblage from the DILM-1 well, central Saudi Arabia, contains very well preserved, relatively small (Text-Figure 7), cells ranging in shape from very regular cylindrical, to flask-shaped, spindle-shaped and ovoid. The cell wall and the inner body wall are relatively thick and usually smooth; the inner body and outer cell are adpressed and difficult to distinguish optically, though a few broken specimens (Plate 5, Fig. 9) allow the relationship between the inner body and outer cell wall to be examined.

3.3.9 Tesero section, Austria

The 4 outcrop samples from the Permian-Triassic boundary beds at Tesero, Austria contain extremely rich assemblages of cells. These are generally small (Text-Figure 7) and range in shape from cylindrical, to flask shaped, ovoid and 'Y' shaped; the cells are commonly joined in long chains of up to 20 (Plate 4).

The cell wall and the inner body wall are relatively thick and usually smooth; the inner body and outer cell are adpressed and difficult to distinguish optically, though a number of specimens show small amounts of detachment between the two wall layers (Plate 4, Figs. 6, 9-10). Rarely specimens indicate high degrees of inner body shrinkage (Plate 4, Fig. 8). As in specimens from other locations, it is clear that detachment of the inner body occurs last from the termini of the cell outer wall.

3.4 PALAEOLATITUDE AND SIZE VARIATIONS IN *R. CHALASTUS*

The scattergram (Text-Figure 7) shows that the largest constituent cells of *R. chalastus* occur in the assemblages from Junggar, China; Kap Stosch, Greenland and the Russian Platform. The palaeogeographical positions of these localities are within the palaeotemperate latitudes (Text-Figure 8). Smaller cells occur in the palaeotropical and paleoequatorial Permian of northern Australia, Saudi Arabia, UK and Austria. This trend may indicate a palaeoenvironmental control on the growth and development of the organism that produced *R. chalastus*.

4 Ages of the material

4.1 AUSTRALIA – BOWEN AND BONAPARTE BASINS

Examples of *R. chalastus* from the Bowen Basin are from type material from the Rewan Formation (Foster, 1979), while those from the Bonaparte Basin, in northern Australia (Text-Figure 8) are from the Blina Shale, intersected in a petroleum exploration borehole, BHPP Billawok 1, studied by Helby (1992).

In both basins, *R. chalastus* occurs in assemblages assigned to the *Protohaploxypinus microcorpus* Zone, as emended by Foster (1982). The age of this zone is controversial, in that some authors regard it as either latest Permian or earliest Triassic, or spanning the boundary (see McLoughlin et al., 1997). In that assemblages from this zone lack *Aratrisporites* spp., Foster et al. (1998) argued for a Late Permian age, but facies may control the first appearance of these spores from one lycopod group. It is nevertheless noteworthy that the downward range of *Aratrisporites* spp. and its inclusion in the *P. microcorpus* Zone in Helby et al. (1987, fig. 5) results from a drafting error (Helby, pers. comm.).

Independent age constraints for the *P. microcorpus* Zone are based on superposition. Faunas associated with palynofloras from the underlying *Dulhuntyispora parvithola* Zone (APP 5; Price, 1997) range in age from Kazanian (Wordian) to Dzhulfian (see Foster and Archbold (2001) for details).

In terms of the Russian Stages, Jones and Chen (2000) suggest a correlation of *D. parvithola*-bearing sediments of the Newcastle Coal Measures, Sydney Basin, eastern Australia, with the Late Tatarian Vjatian horizon (*sic*) of the Russian Platform, based on conchostracan faunas. The youngest age for the *P. microcorpus* Zone relies on palynological correlation, and acceptance of the FAD of *Aratrisporites*, which occurs in marine rocks of early Griesbachian age in the Perth Basin of western Australia (see Dolby and Balme, 1976). On this evidence it it is no younger than early Griesbachian.

Essential elements of the *P. microcorpus* Zone include the eponymous species, *Playfordiaspora cancellosa*, and *Triplexisporites playfordii*, all of which first appear in the immediately underlying *P. cancellosa* (al. *crenulata*) Zone of Foster (1982). Some workers regard the latter zone as a facies variant of the *P. microcorpus* zone (Helby et al.,1987), but what is most important is that since the work of Balme and Helby (1973), Australian workers have used the appearance of these key species to correlate with assemblages from the uppermost Chhidru Formation (Balme, 1970), which on conodont evidence is currently regarded as early Changhsingian (Wardlaw and Pogue, 1995). Thus from palynological evidence an apparently more refined age for the *P. microcorpus* Zone is early Changhsingian.

4.2 KAP STOSCH, GREENLAND

Two samples 750(675)-4 and 750(675)-6 were taken from locality 6.75 (see Balme 1980; p.9, fig. 1), Kap Stosch, East Greenland, but the lithological unit from which the samples came was not identified formally. The assemblages belong to the *Protohaploxypinus* Association which Balme (1980), considered to be earliest Griesbachian on the basis of palynological comparisons with mainland Canada and the Arctic islands, and on the occurrence of *Otoceras woodwardi boreale* Spath and *Glyptophiceras triviale* Spath. Balme (1980) also reported *R. chalastus* from the succeeding Griesbachian *Taeniaesporites* Association. Utting and Piasecki (1995) reported (but did not illustrate) *R. chalastus* (as *T. stoschiana*) from the Karstryggen Formation (correlated with the Capitanian by Henderson & Mei (2000)), and the younger Schuchert Dal Formation which is dated Dzhulfian by ammonoids (Nassichuk 1995). These occurrences indicate that *R. chalastus* has a relatively long stratigraphic range in the region.

4.3 TESERO, AUSTRIA

The three samples T1 6403434, T2 6403435 and T3 6403436, are from a lutite horizon within the Mazzin Member at the Tesero Section, Austrian Alps. The Mazzin Member is separated from the latest Permian Bellerophon Formation by the Tesero Member and the basal Triassic conodont marker species *H. parvus* occurs 130 cm above the base of the Tesero Member in the Bulla Section (Cassinis et al., 2000), and has been reported from the lower Mazzin Member (see Broglio Loriga and Cassinis, 1992) confirming a Triassic age for the Mazzin Member. Based on other included fossils, the Mazzin Member has been assigned a Griesbachian age by Assereto et al. (1973), Broglio Loriga et al. (1983) and Noé (1987).

Recent evidence (Looy et al., in press, see ODP Excursion Field Guide, Italia 2001; p. 95) suggests that 'fungal remains' (?*R. chalastus*) appear to occur over relatively short interval extending approx. 12m below, and approx. 15m above, the Permian-Triassic boundary.

4.4 JUNGGAR, NORTHERN XINJIANG, CHINA

Five samples, 640 3380, 640 3381, 640 3417, 640 3390 and 640 3400 were taken from the lower part of the Guodikeng Formation (Lower Canfanggou Group; see Appendix 1 for sample levels) on both limbs of the Dalongkou anticline. Although the Permian of the Junggar basin is continental and therefore difficult to relate to the marine basal Triassic stratotype section at Meishan, a number of lines of evidence suggest that the Guodikeng Formation spans the Permian-Triassic boundary.

Li et al. (1986) described the palynomorphs, megaspores, megaflora, bivalves, ostracods, conchostracans and vertebrates of the Guodikeng Formation. They considered that all but the top 30m of the Guodikeng Formation is latest Permian in age while the top 30m, and the overlying Jiucaiyuan Formation, are wholly Triassic in age. Li et al. (1986) reported *Alisporites*, *Pteruchipollenites*, *Klausipollenites*, *Protohaploxypinus limpidus*, *P. ovaticorpus*, *Lueckisporites virkkiae*, *Limatulasporites fossulatus*, and *Lundbladispora* in the lower and middle parts of the formation but note an increase in the abundance of spores, accompanied by the appearance of *Taeniaesporites* and *Equiselosporites*, in the upper part of the formation. Li et al. (1986) considered these changes to indicate the onset of the Triassic. Significantly Li et al. (1986) did not record *Aratrisporites* in the Guodikeng Formation but report it from the overlying Jiucaiyuan Formation along with abundant spores including *Lundbladispora nejburgii* and *L. willmotti.* Li et al. (1986) considered that conchostracans in the top 30m of the Guodikeng Formation also indicated a Triassic age.

Ouyang et al. (1999) and Ouyang and Norris (1999) suggested that the top 40-50m of the Guodikeng Formation is Early Triassic in age, on the basis of the occurrence of an assemblage containing *Lundbladispora*, *Aratrisporites* and *Lunatisporites*. Ouyang and Norris (1999) considered that the appearance of *Aratrisporites* has special significance because, based on the palynological work of Ouyang and Utting (1990), its first appearance is 2.7m above the base of the Triassic at Meishan. Ouyang et al. (1999) noted species such as *Lueckisporites virkkiae* and *Scutasporites unicus* (as *S. xinjiangensis*) in the lower and middle parts of the Guodikeng Formation, which they therefore consider to be correlative with the Tatarian of the Russian Platform.

Samples collected for the present study from the lower part of the Guodikeng Formation, confirm the presence of *L. virkkiae* and *Scutasporites* spp.. Conchostracans from the same samples, assigned by Prof Shen Yan-bin, Nanjing Institute, Chinese Academy of Sciences (pers. comm.) to the following species: *Beijianglimnadia* sp., *Bipemphigus* cf. *gennisi* Novozhilov 1965 and *Polygrapta chatangensis* Novozhilov 1946, also suggest a Tatarian age.

Apart from palaeontological evidence, palaeomagnetic evidence (Jin and Shang, 2000) which places the Illawara Reversal within the Lucaogou Formation (of the Upper Jijicao Group, see Ouyang et al., 1999) further suggests that the Upper Jijicao and Lower Canfanggou Groups are Capitanian or younger in age.

Ouyang and Utting (1990) reported *R. chalastus* (as *T. stoschiana*) from the top 40m Changhsing Formation at Meishan, but not from the Griesbachian Chinglung Formation; Ouyang and Norris (1999) noted the presence of *R. chalastus* in the Griesbachian Jiucaiyuan Formation at the Junggar section.

4.5 RUSSIAN PLATFORM

This sample, collected by Dr. O. Yaroshenko, originates from the lower Vetlugian Series at a depth of 44.4m in Borehole No. 453K, 3.5km NE from Shartanovo Village, Vologodskaya Region. The lower part of the Vetlugian on the Russian Platform is correlated with the *Otoceras* and *Ophiceras* zones on the basis of vertebrate, palynological, ostracod and conchostracan evidence (Lozovskiy, 1992) and is therefore Griesbachian in age.

4.6 DILM-1 WELL, SAUDI ARABIA

This sample originates from the informally named 'basal Khuff clastics' at a depth of 7827.9 feet in borehole DILM-1, central Saudi Arabia. Direct dating of this unit is by palynology and palaeobotany only; though some upper limit dates are available from the Khuff Formation above. El-Khayal and Wagner (1985) suggested a Zechstein-equivalent age for the basal Khuff clastics macroflora at the Ash Shuqqah section. Stephenson and Filatoff (2000) considered the basal Khuff clastics to be Tatarian or younger in age (possibly Changhsingian). The lower part of the Khuff (?basal Khuff clastics) in the Hawtah field is dated as Late Tatarian (van der Eem in Al-Jallal (1994)).

4.7 GREER COUNTY, OKLAHOMA, USA

Samples from 66398 and 66399 were collected by Dr B. E. Balme from the Flowerpot Formation of Greer County, Oklahoma. The Flowerpot Formation has been dated on reptile fossil remains as Kazanian in age (Chudinov, 1965).

4.8 HILTON PLANT BEDS, UK

Illustrated specimens from the Hilton Plant Bed are from a palynological strew slide given to one of us (CBF) by Prof. H. Visscher in 1978. Although not illustrated here, Dr G. Warrington has also recorded *R. chalastus* from the Hilton Plant Bed at Hilton Beck, 0.5 miles west of Hilton Village, Cumbria. Clarke (1965) implied a Late Permian 'Zechstein' age for the Hilton Plant Beds on the basis of comparison with palynofloras described by Klaus (1963); Leschik (1956), Grebe and Schweitzer (1962) and Scharschmidt (1963). Stoneley (1958) considered the macroflora of the bed to be of Late Permian 'Thuringian' age. On the basis of recent correlation using conodonts Henderson and Mei (2000) have suggested a Wuchiapingian age for the Zechstein.

4.9 CONISBOROUGH, UK

Sample 73862 was collected by Dr. B. E. Balme from a 'grey claystone of the Lower part of the Permian succession above the Carboniferous' at Conisborough, Yorkshire, UK. Balme correlated the assemblage with those of the Zechstein (pers. comm.) which implies a possible Wuchiapingian age for the assemblage (Henderson and Mei, 2000).

4.10 SUMMARY OF AGE INFORMATION

The ages suggested for the localities studied and for other published occurrences of *R. chalastus* and *R. catenulatus* are summarised in Text-Figure 9. The ranges indicate that although *R. catenulatus* has a restricted stratigraphic range, that of *R. chalastus* is relatively long, spanning at least 10 Myr in the Permian (Capitanian-Chansinghian) and continuing into the Early Triassic. Significantly its range is not restricted to the narrow sections spanning Permian-Triassic boundary.

5 Geochemical analysis

The carbon isotopic composition ($d^{13}C$) of *R. chalastus*, and of its apparent food sources, suggests it is not a saprophyte. Moreover the wall composition of *R. chalastus*, determined by gas chromatography mass spectrometry (GCMS) and micro -Fourier Transform Infrared Spectroscopy (micro-FTIR), is consistent with that of an alga.

The palynological assemblage from the Werfen Formation (T1 6403434) is almost entirely made up of *R. chalastus*, but was further concentrated by using a +25 µm sieve fraction, and the purity then confirmed using a low power objective. The $d^{13}C$ isotopic composition of *R. chalastus* is -32‰. If *R. chalastus* was a saprophyte living on decaying vegetation, its isotopic composition would be slightly heavier than its food source (Koch et al., 1994) Our studies of potential food sources (for the supposed saprophyte), of both woody tissue and pollen from the underlying Late Permian Groedner Sandstone, show a $d^{13}C$ isotopic composition of -22‰, which is significantly heavier. Thus it is unlikely that *R. chalastus* was a saprophytic organism deriving its energy from woody tissue and pollen.

Because our specimens of *R. chalastus* are from the Early Triassic Werfen Formation it might argued that they should depleted isotopically in $d^{13}C$, as a result of secular change. However, older, Late Permian assemblages with *R. chalastus* from the Junggar Basin (this study) are also depleted in $d^{13}C$, with values of -30 to -33‰.

The molecular composition of the wall material of *R. chalastus* was investigated by micro-FTIR and pyrolysis GCMS. The fossils were first cleaned by either mild thermal treatment or the use of organic solvents (acetone or dichloromethane) to remove extraneous surface adsorbed organic matter. The FTIR analysis was performed with a magna-IR 760 equipped with a Nicolet microscope and the signal from the material was characterised by prominent hydroxyl, aliphatic and carbonyl groups. Aliphatic C-H bands present included symmetric and asymmetric vibrations at 2930 cm^{-1} (*vas* CH_2 + CH_3), 2850 cm^{-1} (*vs* CH_2+CH_3) and deformational vibrations at 1450 cm^{-1} (?CH_2) and 1380 cm^{-1} (?CH_2) (Text-Figure 10).

Pyrolysis was performed on ~0.3mg of fossils at 600°C/10s using a CDS (Chemical Data Systems Inc) pyroprobe interfaced to a HP 6890/5973 GCMS. The products were detected by monitoring selected ions diagnostic of common compound classes. The main aliphatic pyrolysates produced were a homologous series of *n*-alkenes/alkanes from C_8 to ~C_{21} (Text-Figure 11a). The *n*-alkenes are products of the open pyrolysis process and arise from the same saturated long chain macromolecular precursors as the *n*-alkanes. These straight chain compounds most likely account for the aliphatic C-H bands measured by FTIR. They are similar, although of relatively shorter average chain length, to the *n*-alkene/alkane series typically detected from the highly aliphatic biomacromolecule ‘algaenan’ of many species of Chlorophyceae (Tegelaar et al., 1989; see also Al-Arouri et al., 1999 for discussion of specific examples) and are attributed to a macromolecular structure based on polymethylenic chains, linked primarily via ether bonds.

Several distributions of aromatic pyrolysates were also detected in high abundance (Text-Figure 11b). These included alkylbenzenes, alkylnaphthalenes and alkylphenols, the latter group are also reflected by the large –OH band measured by FT-IR (3400 cm^{-1}). Alkylphenols are not particularly source specific, but have been detected from various types of algae as well as higher order plants, lignin and even melanoidin like compounds (see Al-Arouri et al., 1999 for more comprehensive discussion). The absence of methoxyphenols and isoprenoids suggests there is minimal lignin and melanoidin input, respectively. Akylbenzenes are usually the main aromatic products detected from algaenan, but typically in low concentration relative to aliphatic hydrocarbons. Their high relative abundance may be due to the antiquity (approx. 250 Ma) of these fossils or alternatively may reflect non-indigenous organic material that was not removed by the pre-treatment procedures.

The presence of algaenan biomacromolecules is indicative of an algal origin. Furthermore, the results show little specific evidence for fungal biopolymers such as cellulose, mannans and/or glucans.

The biogeochemical data, presented here, strongly supports an algal origin for *R. chalastus.*

6 Conclusions

1. *Chordecystia* Foster 1979 and *Tympanicysta* Balme 1980 are junior synonyms of *Reduviasporonites* Wilson 1962.
2. *Reduviasporonites stoschianus* (Balme) Elsik 1999 is a junior synonym of *Reduviasporonites chalastus* (Foster) Elsik 1999. *Reduviasporonites catenulatus* Wilson 1962 differs from *R. chalastus* in being smaller, in having more rounded constituent cells and in having less well developed terminal rims.
3. *Brazilea helbyi* forma *gregata* Foster 1979, recorded only from the type material of *R. chalastus,* may also be a junior synonym of *R. chalastus.*
4. The size of the constituent cells present in *R. chalastus* appears to be related to palaeolatitude, with large examples occurring in the palaeotemperate Permian of China, Russia, Sverdrup and Moura, Australia and smaller cells occurring in the palaeotropical and paleoequatorial Permian of northern Australia, Saudi Arabia, UK and Austria.
5. The stratigraphical occurences of the species of *Reduviasporonites* suggest that *R. catenulatus* is most common in the Wordian (Kazanian) of Oklahoma, though specimens of the size range associated with *R. catenulatus* are present very rarely in the Austrian Mazzin Member. *R. chalastus* occurs in Late Permian and Early Triassic rocks but may be present outside narrow sequences spanning the Permian-Triassic boundary.
6. Geochemical evidence suggests that *R. chalastus* is algal rather than fungal in origin.
7. *R. chalastus* is unlikely to be integral to the process of mass extinction occurring at or near the Permian-Triassic boundary as suggested by Eshet et al. (1995) and Visscher et al. (1996) because

? it appears to range outside the postulated time of the mass extinction,

? as a probable alga rather than a fungus, it cannot have acted as a saprophytic metaboliser of dead vegetation formed in the extinction event.

References

AL-AROURI, K., GREENWOOD, P. F and WALTER, M. 1999. A possible chlorophycean affinity of some Neoproterozoic acritarchs. *Organic Geochemistry*, 30: 1323-1337.

AL-JALLAL, I. A. 1994. The Khuff Formation: its regional reservoir potential in Saudi Arabia and other Gulf countries; depositional and stratigraphic approach. *In:* Al-Husseini, M. I. (ed.) *Geo 1994, Middle East Geoscience Conference*, April 25-27, 1994, Vol 1, Gulf Petrolink, Bahrain: 103-119.

ASSERETO, R., BOSELLINI, A., FANTINI SESTINI, N. & SWEET, W. C. 1973. The Permian-Triassic boundary in the southern Alps (Italy). *In*: Logan, A. & Hills, L. V. (eds.) *The Permian and Triassic systems and their mutual boundary*, Canadian Society of Petroleum Geologists (Memoir 2), Calgary, Alberta: 176-199.

BALME, B. E. 1970. Palynology of Permian and Triassic Strata in the Salt Range and Surghar Range, West Pakistan. *In*: Kummel, B. and Teichert, C. (eds.) *Stratigraphic boundary problems:*

Permian and Triassic of West Pakistan. University Press of Kansas, Department of Geology Special Publication 4: 306-453.

BALME, B. E. 1980. Palynology of Permian-Triassic boundary beds at Kap Stosch, east Greenland. *Meddelelser om Grønland, udgivne af kommissionnen for Kidenskabelige Undersøgelser i Grønland*, 200: 1-37.

BALME, B. E. and HELBY, R. J. 1973. Floral modifications at the Permian-Triassic boundary in Australia. *In*: Logan, A. & Hills, L. V. (eds.) T*he Permian and Triassic systems and their mutual boundary*, Canadian Society of Petroleum Geologists (Memoir 2), Calgary, Alberta: 433-444.

BROGLIO LORIGA, C. and CASSINIS, G. 1992. The Permo-Triassic boundary in the southern Alps (Italy) and in Periadriatic regions. *In:* Sweet, W. C. Zunyi, Y, Dickens, J. M., Hongfu, Y. (eds.) *Permo-Triassic events in the eastern Tethys*, Cambridge University Press: 78-97.

BROGLIO LORIGA, C., GÓCZÁN, F., HAAS, J. LENNER, K., NERI, C., ORAVECZ S., POSENATO, R., SZABÓ, I. and TÓTH MAKK, Á. 1990. The Lower Triassic sequences of the Dolomites (Italy) and the Transdanubian Mid-Mountains (Hungary) and their correlation. *Memorie di Scienze Geologiche, Universita di Padova*, 17: 41-103.

BROGLIO LORIGA, C., MASETTI, D. and NERI, C. 1983. La Formazione di Werfen (Scitico) delle Dolomiti Occidentali: sedimentologia e biostratigrafia. . Rivista Italiana di Paleontologia e Stratigrafia., 88, 501-598.

CASSINIS, G., DI SEFANO, P., MASSARI, F., NERI, C. and VENTURINI, C. 2000. Permian of south Europe and its interregional correlation. *In:* Yin, H., Dickens, J. M., Shi, G. R. & Tong, J. (eds.) *Permian-Triassic Evolution of Tethys and Western Circum-Pacific*, Elsevier: 37-70.

CHUDINOV, P. K. 1965. New facts about the fauna of the Upper Permian of the USSR. *Journal of Geology*, 73: 117-130.

CLARKE, R. F. A. 1965. British Permian saccate and monosulcate miospores. *Palaeontology*, 8: 322-354.

DOLBY, J. H. and BALME, B. E. 1976. Triassic palynology of the Carnarvon Basin, Western Australia. Review of Palaeobotany and Palynology, 22: 105-168.

EL-KHAYAL, A. A. and WAGNER, R. H. 1985. Upper Permian stratigraphy and megafloras of Saudi Arabia: palaeogeographic and climatic implications. *Compte Rendu 10th International Congress on Carboniferous Stratigraphy and Geology* (Madrid 1983), 3: 17-26.

ELSIK, W. C. 1999. *Reduviasporonites* Wilson 1962: synonymy of the fungal organism involved in the Late Permian crisis. *Palynology*, 23: 37-41.

ERWIN, D. H. 1993. *The Great Paleozoic Crisis: life and death in the Permian*. Columbia University Press, New York, 327 p.

ESHET, Y., RAMPINO, M. R. and VISSCHER, H. 1995. Fungal event and palynological record of ecological crisis and recovery across the Permian-Triassic boundary. *Geology*, 23: 967-970.

FOSTER, C. B. 1979. Permian Plant Microfossils of the Blair Atholl Coal Measures, Baralaba Coal Measures and Basal Rewan Formation of Queensland. *Geological Survey of Queensland Publications*, 372: 1-244.

FOSTER, C. B. 1982. Spore-pollen assemblages of the Bowen Basin, Queensland (Australia): Their relationship to the Permian-Triassic boundary. *Review of Palaeobotany and Palynology* 36: 165-183.

FOSTER, C. B. and ARCHBOLD, N. W. 2001. Chronologic anchor points for the Permian and Early Triassic of the eastern Australian basins. *In:* Weiss, R. E. (ed.) *Contributions to geology*

and paleontology of Gondwana – in honour of Helmut Hopfner, Geological Institute, University of Cologne: 175-199.

FOSTER, C. B., LOGAN, G. A. and SUMMONS, R. E. 1998. The Permian-Triassic boundary in Australia: where is it and how is it expressed? *Proceedings of the Royal Society of Victoria,* 110: 247-266.

GREBE, H. and SCHWEITZER, H-J. 1962. Die sporae dispersae des niederrheinischen Zechsteins. Vorausdruck Fortschritte in der Geologie von Rheinland und Westfalen, 10: 1-24.

HANKEL, O. 1992. Late Permian to early Triassic microfloral assemblages from Maji ya Chumvi Formation, Kenya. *Review of Palaeobotany and Palynology,* 72: 129-147.

HELBY R., 1992. BHP Petroleum Billawock – 1, Palynological Report, 13pp + 2 charts (unpublished).

HELBY, R., MORGAN, R. and PARTRIDGE, A. D. 1987. A palynological zonation of the Australian Mesozoic. Memoirs of the Association Australasian. Palaeontologists, 4: 1-94.

HENDERSON, C. M. and MEI, M. 2000. Preliminary cool water Permian Conodont Zonation in north Pangea: a review. *Permophiles,* No. 36, 16-23.

JIN, Y. and SHANG, Q. 2000. The Permian of China and its interregional correlation. *In:* Yin, H., Dickins, J. M., Shi, G. R. & Tong, J. (eds.) *Permian-Triassic evolution of Tethys and Western Circum-Pacific,* Elsevier: 71-98.

JIN, Y., WARDLAW, B. R., GLENISTER, B. F. and KOTLYAR, G. V. 1997. Permian chronostratigraphic subdivisions. *Episodes,* 20, 10-15.

JONES, P. J. and CHEN, Pei-ji 2000. Carboniferous and Permian Leaioidea (Branchiopoda: conchostraca) from Australia: taxonomic revision and biostratigraphic implications. *Records of the Australian Museum,* 52: 223-244.

KILANI-MAZRAOUI, F., RAZGALLAH-GARGOURI, S. and MANNAI-TAYECH, B. 1990. The Permo-Triassic of Southern Tunisia - Biostratigraphy and palaeoenvironment. *Review of Palaeobotany and Palynology,* 66: 73-291.

KLAUS, W. 1963. Sporen aus dem südalpinen Perm. *Jahrbuch der Geologischen Bundesanstalt*, Wien, 106: 229-363.

KOCH, P. H., FOGEL, M. L. and TUROSS, N. 1994 Tracing the diets of fossil animals using stable isotopes *In* Lajtha, K. & Mitchener, R. H., (eds.), *Stable isotopes in ecology and environmental science,* Blackwell, Oxford, p. 63-92.

KRASSILOV, V. A., AFONIN, S. A. and BARINOVA, S. S. 1999. *Tympanicysta* and the terminal Permian events. *Permophiles* No. 35, 16-17.

LESCHIK, G. 1956. Sporen aus dem Salzton des Zechsteins von Neuhof (bei Fulda). *Palaeontographica* B, 100: 122-142.

LI, P. X., ZHANG, Z. M. and WU, S. Z. 1986. Stratigraphy. In: Permian and Triassic strata and fossil assemblages in the Dalongkou area of Jimsar, Xinjiang. Geological Memoir Series 2, Geological Publishing House, Beijing: 2-38 (in Chinese with English summary).

LOZOVSKIY, V. R. 1992. The Permian-Triassic boundary in continental series of Laurasia and its correlation with the marine scale. *International Geology Review,* 34: 1008-1014.

LOZOVSKY, V.R. and ESAULOVA, N.K. 1998 . *Granitsa permi i triasa v kontinental'nykh seriyakh Vostochnoy Evropy (Permian-Triassic Boundary in the Continental Series of East Europe)*. Moscow, GEOS Press, 219 pgs (in Russian).

MANGARUD, G. and KONIECZNY, R. M. 1993. Palynology of the Permian succession of Spitzbergen, Svalbard. *Polar Research,* 12: 65-93.

MANGARUD, G. 1994. Palynostratigraphy of the Permian and lowermost Triassic succession, Finnmark Platform, Barents Sea. *Review of Palaeobotany and Palynology*, 82: 317-349.

MCLOUGHLIN, S., LINDSTRÖM, S. and DRINNAN, A. N. 1997. Gondwana floristic and sedimentological trends during the Permian-Triassic transition: new evidence from the Amery Group, northern Prince Charles Mountains, East Antarctica. *Antarctic Science*, 9: 281-298.

MORGAN, B. E. 1967. Palynology of a portion of the El Reno Group (Permian), southwest Oklahoma. *Unpublished PhD thesis*, University of Oklahoma.

NADER, A. D., KHALAF, F. H. and HADID, A. A. 1993. Palynology of the Permo-Triassic boundary in Borehole Mityah-1, south west Mosul City, Iraq. *Mu'tah Journal of Research and Studies*, 8: 223-280.

NASSICHUK, W. W. 1995. Permian ammonoids in the Arctic regions of the world. *In*: Scholle, P. A., Peryt, T. M. & Ulmer-Scholle, D. S.. (eds.) *The Permian of Northern Pangea Vol. 1. Palaeogeography, Palaeoclimates, Stratigraphy*, Springer Verlag: 210-235.

NOÉ, S. U., 1987. Facies and paleogeography of the marine Upper Permian and of the Permian-Triassic boundary in the southern Alps (Bellerophon Fm., Tesero Horizon). *Facies*, 16: 89-142.

OUYANG, S. and NORRIS, G. 1999. Earliest Triassic (Induan) spores and pollen from the Junggar Basin, Xinjiang, northwestern China. *Review of Palaeobotany and Palynology*, 106: 1-56.

OUYANG, S. and UTTING, J. 1990. Palynology of Upper Permian and Lower Triassic rocks, Meishan, Changxing County, Zhejiang Province, China. *Review of Palaeobotany and Palynology*, 66: 65-103.

OUYANG, S., ZHOU, Y., WANG, Z. and ZHAN, J. 1999. Palynostratigraphic correlation of the Permian System of Northern Xinjiang and the Cis-Urals. *Permophiles* No. 33, 24-27.

PRICE, P. L. 1997. Permian to Jurassic palynostratigraphic nomenclature of the Bowen and Surat basins. *In*: Green, P. (ed.) *The Surat and Bowen Basins, southeast Queensland*, Queensland Department of Mines and Energy, Brisbane: 137-178.

SCHAARSCHMIDT, F. 1963. Spores und hystricosphaerideen aus dem Zechstein von Büdingen in der Wetterau. *Palaeontographica* B, 113: 38-91.

STEPHENSON, M. H. & FILATOFF, J. 2000. Description and correlation of Late Permian palynological assemblages from the Khuff Formation, Saudi Arabia and evidence for the duration of the pre-Khuff hiatus. *In*: Al-Hajri, S. & Owens, B. (eds.) *Stratigraphic palynology of the Palaeozoic of Saudi Arabia*, Gulf Petrolink, Bahrain GeoArabia Special Publication No. 1, 192-215.

STONELEY, H. M. M. 1958. The Upper Permian flora of England. Bulletin of the British Museum (Natural History), 3, 293-337.

TEGELAAR, E. W., DE LEEUW, J. W., DERENNE, S and LARGEAU, C. 1989. A reappraisal of kerogen formation. *Geochimica et Cosmochimica Acta* 52: 2625-2637.

UTTING, J. and PIASECKI, S. 1995. Palynology of the Permian of northern Continents: a review. *In*: Scholle, P. A., Peryt, T. M. & Ulmer-Scholle, P. A. (eds.) *The Permian of Northern Pangea Vol. 1. Palaeogeography, Palaeoclimates, Stratigraphy*, Springer Verlag, 236-261.

UTTING, J. 1994. Palynostratigraphy of Permian and Lower Triassic rocks, Sverdrup Basin, Canadian Arctic Archipelago. *Geological Survey of Canada Bulletin* 478: 1-107.

VISSCHER, H., BRINKHUIS, H., DILCHER, D. L., ELSIK, W. C., ESHET, Y., LOOY, C., RAMPINO, M. R. and TRAVERSE, A. 1996. The terminal Paleozoic fungal event: evidence of terrestial ecosystem destabilisation and collapse. *Proceedings of the National Academy of Sciences* USA, 93: 2155-21.

WARDLAW, B. R. and POGUE, K. R. 1995. The Permian of Pakistan. *In:* Scholle, P. A., Peryt, T. M. & Ulmer-Scholle, D. S. (eds.) *The Permian of Northern Pangea Vol. 1 Palaeogeography, Palaeoclimates, Stratigraphy*. Springer Verlag: 215-224.

WILSON, L. R. 1962. A Permian fungus spore type from the Flowerpot Formation of Oklahoma. *Oklahoma Geology Notes*, 22: 91-96.

WOOD, G. D. and ELSIK, W. C. 1999. Paleoecologic and stratigraphic importance of the fungus *Reduviasporonites stoschianus* from the 'Early-Middle' Pennsylvanian of the Copacabana Formation, Peru. *Palynology*, 23: 43-53.

WRIGHT, R. P. and ASKIN, R. A. 1987. The Permian-Triassic Boundary in the southern Morondava Basin of Madagascar. *In:* Mackenzie, C. D. (ed.) *Gondwana 6 Stratigraphy, Sedimentology and Palaeontology*. American Geophysical Union Geophysical Monograph, 41: 157-166.

ZIEGLER, A. M., HULVER, M. L. and ROWLEY, D. B. 1997. Permian world topography and climate. *In:* Martini, I. P. (ed.) *Late glacial and postglacial environmental changes*, OUP: 111-146.

7 Captions for figures

7.1 TEXT-FIGURE 1

Terminology.

7.2 TEXT-FIGURE 2

Shapes of cells in *R. chalastus* and *R. catenulatus.* (1) basic cylindrical cell, (2) Ovoid cell, (3) Spherical cell, (4) Flask shaped cell with narrow protuberant terminal rims, (5) Ovoid cell with narrow protuberant terminal rims, (6) 'Y' shaped cell with three terminal rims, (7) Spindle shaped cell with protuberant terminal rims and 'striations', (8) Cell forms in *R. catenulatus.*

7.3 TEXT-FIGURE 3

Shrinkage of inner body in the cell cavity. (1) inner body occupies most of the cell, (2) inner body shrunk but attached at both ends to the inner surface of the outer cell wall, (3) inner body in advanced state of shrinkage; envelopes cell material, (4) inner body absent.

7.4 TEXT-FIGURE 4

Fold patterns in *R. chalastus*. (1) Diagonal folds in the outer wall of the cell. Interpreted as being caused by twisting of the terminal rims in opposing directions, (2) Diagonal folds in the inner wall of the cell, (3) Folds or dark areas interpreted as being caused by residual adpression of inner body to the outer cell wall or by folding in the inner body. Folds may therefore delineate the position of the inner body when it is not visible, (4) Folds close to the margins of ovoid cells, and orientated perpendicular to the long axis of the cell, are believed to result from the attachment of the termini of the inner body to the inner surface of the outer body and as such may represent parts of a poorly developed terminal rim.

7.5 TEXT-FIGURE 5

Fold patterns in *R. catenulatus.* (1) pair of joined cells, (2) single cell.

7.6 TEXT-FIGURE 6

Chain formations in (1) *R. catenulatus* and (2) *R. chalastus.*

7.7 TEXT-FIGURE 7

Scattergram of the lengths and widths of cells from *R. catenulatus* and *R. chalastus.*

Key: Green dots = specimens of *R. catenulatus* from the Flowerpot Formation; Red dots = Austrian specimens of *R. chalastus*; mauve dots = Saudi Arabian specimens of *R. chalastus*; red squares = British specimens (Conisborough) of *R. chalastus*; green crosses = Australian (Billawock) specimens of *R. chalastus*; blue 'z' = Russian specimens of *R. chalastus*; dark blue crosses = Chinese specimens of *R. chalastus*; yellow 'Y' = Australian (Moura) specimens of *R. chalastus*; purple triangles British specimens (Hilton Plant Beds) of *R. chalastus*; green diamonds Greenland specimens of *R. chalastus.*

7.8 TEXT-FIGURE 8

Palaeogeographic map showing positions of the samples studied. Map and sample positions based on Ziegler et al. (1996). (1) Junggar, Northern Xinjiang, China, (2) Russian Platform, (3) Kap Stosch, Greenland, (4) Conisborough and Hilton Plant Beds, UK, (5) Tesero, Austria, (6) DILM-1, central Saudi Arabia, (7) Billawock, Bonaparte basin, Australia, (8) Moura, Bowen Basin, Australia.

7.9 TEXT-FIGURE 9

Table of ages suggested for the localities studied and for other published occurrences of *R. chalastus* and *R. catenulatus*. The correlation of the 'standard', 'traditional' and 'Tethys' scales is based on that suggested by Jin et al. (1997). In the case of other published studies, ages given by the authors are given at face value. The relationship of 'fungal remains' assigned to *Reduviasporonites stoschianus* (Balme) Elsik 1999 by Wood & Elsik (1999) to other species of *Reduviasporonites* is doubtful. Therefore this occurrence has not been included in the diagram.

7.10 TEXT-FIGURE 10

FT-IR spectra of *R. chalastus*. Major aliphatic signals are observed at 2800-3000 and 1300-1500cm^{-1}.

7.11 TEXT-FIGURE 11

(a) reconstructed m/z 57 and (b) TIC from the 600^0C pyroprobe GC-MS analysis of *R. chalastus*. Cn= n-alkane; B=benzene (B1=methylbenzene); P=phenol; N=naphthalene; DBF=dibenzofuran.

8 Plate descriptions

Illustrated specimens are housed in the Commonwealth Palaeontological Collection at AGSO – Geoscience Australia, and are assigned a unique catalog number prefixed CPC. Details regarding sample locality and location of specimens on strew slides are given in Appendix 1.

8.1 PLATE 1:

All specimens photographed using DIC; scale bar is 25 micrometres.

Figs. 1 to 7 *R. chalastus* (Foster) Elsik 1999 from BHPP Billawock No. 1, offshore Bonaparte Basin, Australia.

Figs. 8-18 *R. chalastus* (Foster) Elsik 1999 from Borehole N. S. 30 (Moura), Bowen Basin, Queensland, Australia.

Fig.1 – CPC 36673

Fig. 2 – CPC 36674

Fig. 3 – CPC 36675

Fig. 4 – CPC 36676

Fig. 5 – CPC 36677

Fig. 6 – CPC 36676 (detail of Fig. 4)

Fig. 7 – CPC 36677 (detail of Fig. 5)

Fig. 8 – CPC 36678

Fig. 9 – CPC 36679

Fig. 10 – CPC 36680

Fig. 11 – CPC 36681

Fig. 12 – CPC 36682

Fig. 13 – CPC 36683

Fig. 14 – CPC 36684

Fig. 15 – CPC 36685

Fig. 16 – CPC 36686

Fig. 17 – CPC 36687

Fig. 18 – CPC 36688

8.2 PLATE 2:

All specimens photographed using DIC; scale bar is 25 micrometres.

Figs. 1 to 10 *R. chalastus* (Foster) Elsik 1999 from Outcrop Locality 6.75 (see Balme 1980; p.9, fig. 1), Kap Stosch, East Greenland.

Figs. 11, 16-18 *R. chalastus* from Hilton Beck, UK.

Figs. 12-15 *R. chalastus* from outcrop at Conisborough, UK.

Fig.1 – CPC 36689

Fig. 2 – CPC 36690

Fig. 3 – *CPC 36691*

Fig. 4 – CPC 36692

Fig. 5 – CPC 36693

Fig. 6 – CPC 36690 (detail of Fig. 2)

Fig. 7 – CPC 36694

Fig. 8 – CPC 36695

Fig. 9 – CPC 36696

Fig. 10 – CPC 36697

Fig. 11 – CPC 36698

Fig. 12 – CPC 36699

Fig. 13 – CPC 36700

Fig. 14 – CPC 36701

Fig. 15 – CPC 36702

Fig. 16 – CPC 36703

Fig. 17 – CPC 36704

Fig. 18 – CPC 36705

8.3 PLATE 3:

All specimens photographed using DIC, except Figs. 5 and 6 which are SEM microphotographs; Fig. 5 scale bar = 20 micrometers, Fig. 6 scale bar = 50 micrometers; all other scale bars are 25 micrometres.

Fig. 10 *R. chalastus* (Foster) Elsik 1999 from outcrop approximately 192.5m below the top of the Guodikeng Formation, north limb of the Dalongkou Anticline, Junggar, Northern Xinjiang, China. All other figures *R. chalastus* from outcrop approximately 170.5m below the top of the Guodikeng Formation, north limb of the Dalongkou Anticline.

Fig.1 – CPC 36706

Fig. 2 – CPC 36707

Fig. 3 – CPC 36708

Fig. 4 – CPC 36709

Fig. 5 – CPC 36710

Fig. 6 – CPC 36711

Fig. 7 – CPC 36712 showing detached terminal rim.

Fig. 8 – CPC 36713

Fig. 9 – CPC 36714

Fig. 10 – CPC 36715

Fig. 11 – CPC 36707 (detail of Fig. 2)

Fig. 12 – CPC 36707 (detail of Fig. 2)

Fig. 13 – CPC 36716

Fig. 14 – CPC 36717

Fig. 15 – CPC 36718

8.4 PLATE 4:

Figs. 1-10 are photographed using DIC, Figs. 11-15 are scanning electron microphotographs; Figs. 1-10 scale bars are 25 micrometres; Fig. 11 scale bar = 2 micrometers; Fig. 12 scale bar = 5 micrometers; Figs. 13 and 14 scale bars = 20 micrometers; Fig. 15 scale bar = 2 micrometers.

Figs. 1 - 4 *R. chalastus* (Foster) Elsik 1999 from 44.4m depth, Borehole No. 453K, 3.5km, NE from Shartanovo Village, Vologodskaya Region, Russia.

Figs. 5-15 *R. chalastus* from Lutite horizon within the Mazzin Member at the Tesero Section, Austrian Alps.

Fig.1 – CPC 36719

Fig. 2 – CPC 36720

Fig. 3 – CPC 36721

Fig. 4 – CPC 36722

Fig. 5 – CPC 36723

Fig. 6 – CPC 36724

Fig. 7 – CPC 36725

Fig. 8 – CPC 36726

Fig. 9 – CPC 36727

Fig. 10 – CPC 36728

Fig. 11 – CPC 36729

Fig. 12 – CPC 36730

Fig. 13 – CPC 36731

Fig. 14 – CPC 36732

Fig. 15 – CPC 36733 showing break in the cell wall.

8.5 PLATE 5:

Figs. 1-12 are photographed using DIC, Figs. 13-15 are scanning electron microphotographs; Figs. 1-12 scale bars are 25 micrometres; Fig. 13 scale bar = 5 micrometers; Figs. 14 and 15 scale bars = 20 micrometers.

Figs. 1-15 *R. chalastus* (Foster) Elsik 1999 from core sample from depth 7827.9', Borehole DILM-1, central Saudi Arabia.

Fig.1 – CPC 36734

Fig. 2 – CPC 36735

Fig. 3 – CPC 36736

Fig. 4 – CPC 36737

Fig. 5 – CPC 36738

Fig. 6 – CPC 36739

Fig. 7 – CPC 36740

Fig. 8 – CPC 36741

Fig. 9 – CPC 36742

Fig. 10 – CPC 36743

Fig. 11 – CPC 36744

Fig. 12 – CPC 36745

Fig. 13 – CPC 36746 showing detail of terminal rim.

Fig. 14 – CPC 36747

Fig. 15 – CPC 36748

8.6 PLATE 6:

All specimens are photographed using DIC; scale bar for all figures is 25 micrometres.

Figs. 1 to 36 *R. catenulatus* from outcrop samples from Greer County, Oklahoma, USA.

Fig.1 – CPC 36749

Fig. 2 – CPC 36750

Fig. 3 – CPC 36751

Fig. 4 – CPC 36752

Fig. 5 – CPC 36753

Fig. 6 – CPC 36754

Fig. 7 – CPC 36755

Fig. 8 – CPC 36756

Fig. 9 – CPC 36757

Fig. 10 – CPC 36758

Fig. 11 – CPC 36759

Fig. 12 – CPC 36760

Fig. 13 – CPC 36761

Fig. 14 – CPC 36762

Fig. 15 – CPC 36763

Fig. 16 – CPC 36764

Fig. 17 – CPC 36765

Fig. 18 – CPC 36766

Fig. 19 – CPC 36767

Fig. 20 – CPC 36768

9 Authors

C. B. FOSTER, Geoscience Australia, PO Box 378, Canberra ACT, Australia 2061, Email: clinton.foster@ga.gov.au

M. H. STEPHENSON, British Geological Survey, Keyworth, Nottingham, NG12 5GG, UK. Email: m.stephenson@bgs.ac.uk

C. MARSHALL, University of Technology Sydney, Sydney, Australia

G. A. LOGAN, Geoscience Australia, PO Box 378, Canberra ACT, Australia 2061

P. GREENWOOD, Geoscience Australia, PO Box 378, Canberra ACT, Australia 2061

10 Appendix

Plate 1

Figure number	Species	Locality	Depth (m)	Slide	England Finder Co-ordinates	CPC Number
1	*R. chalastus*	BHPP Billawock No.1 offshore Bonaparte Basin	262	Urgen 29.2	J46/2	36673
2	*R. chalastus*	BHPP Billawock No.1 offshore Bonaparte Basin	262	SGM2	O53	36674
3	*R. chalastus*	BHPP Billawock No.1 offshore Bonaparte Basin	262	Urgen 29.2	K46/1	36675
4	*R. chalastus*	BHPP Billawock No.1 offshore Bonaparte Basin	262	SGM4	T39/3	36676
5	*R. chalastus*	BHPP Billawock No.1 offshore Bonaparte Basin	262	SGM5	M39/1	36677
6	*R. chalastus*	BHPP Billawock No.1 offshore Bonaparte Basin	262	SGM4	T39/3 (detail of Fig.4)	36676
7	*R. chalastus*	BHPP Billawock No.1 offshore Bonaparte Basin	262	SGM5	M39/1 (detail of Fig.5)	36677
8	*R. chalastus*	Borehole N.S.30 (Moura), Bowen Basin, Queensland	37.62	MFP 9801/2	P36	36678
9	*R. chalastus*	Borehole N.S.30 (Moura), Bowen Basin, Queensland	37.62	MFP 9801/2	N31	36679
10	*R. chalastus*	Borehole N.S.30 (Moura), Bowen Basin, Queensland	37.62	MFP 9801/1	U46/3	36680
11	*R. chalastus*	Borehole N.S.30 (Moura), Bowen Basin, Queensland	37.62	MFP 9801/2	D51/2	36681
12	*R. chalastus*	Borehole N.S.30 (Moura), Bowen Basin, Queensland	37.62	MFP 9801/1	P33/4	36682
13	*R. chalastus*	Borehole N.S.30 (Moura), Bowen Basin, Queensland	37.62	MFP 9801/2	S44	36683
14	*R. chalastus*	Borehole N.S.30 (Moura), Bowen Basin, Queensland	37.62	MFP 9801/2	O50	36684
15	*R. chalastus*	Borehole N.S.30 (Moura), Bowen Basin, Queensland	37.62	MFP 9801/1	U42	36685
16	*R. chalastus*	Borehole N.S.30 (Moura), Bowen Basin, Queensland	37.62	MFP 9801/2	N46/1	36686
17	*R. chalastus*	Borehole N.S.30 (Moura), Bowen Basin, Queensland	37.62	MFP 9801/2	O48/1	36687
18	*R. chalastus*	Borehole N.S.30 (Moura), Bowen Basin, Queensland	37.62	MFP 9801/2	S36	36688

Plate 2

Figure number	Species	Locality	Slides	England Finder Co-ordinates	CPC Number
1	*R. chalastus*	Locality 6.75 (Balme 1980), Kap Stosch, East Greenland	MFP 12114/3, 750-6	A52/3	36689
2	*R. chalastus*	Locality 6.75 (Balme 1980), Kap Stosch, East Greenland	MFP 12114/3, 750-6	B9	36690
3	*R. chalastus*	Locality 6.75 (Balme 1980), Kap Stosch, East Greenland	MFP 12114/3, 750-6	J21/2	36691
4	*R. chalastus*	Locality 6.75 (Balme 1980), Kap Stosch, East Greenland	MFP 12114/3, 750-6	E24/1	36692
5	*R. chalastus*	Locality 6.75 (Balme 1980), Kap Stosch, East Greenland	MFP 12114/3, 750-6	J36/1	36693
6	*R. chalastus*	Locality 6.75 (Balme 1980), Kap Stosch, East Greenland	MFP 12114/3, 750-6	B9 (detail of Fig. 2)	36690
7	*R. chalastus*	Locality 6.75 (Balme 1980), Kap Stosch, East Greenland	MFP 12114/3, 750-6	E6	36694
8	*R. chalastus*	Locality 6.75 (Balme 1980), Kap Stosch, East Greenland	MFP 12114/3, 750-6	F23/1	36695
9	*R. chalastus*	Locality 6.75 (Balme 1980), Kap Stosch, East Greenland	MFP 12114/3, 750-6	E17	36696
10	*R. chalastus*	Locality 6.75 (Balme 1980), Kap Stosch, East Greenland	MFP 12114/3, 750-6	E35	36697
11	*R. chalastus*	Conisborough, UK	5031	H47/2	36698
12	*R. chalastus*	Hilton Beck, UK	HIL 01	N26/2	36699
13	*R. chalastus*	Hilton Beck, UK	HIL 01	D30/2	36700
14	*R. chalastus*	Hilton Beck, UK	HIL 01	G28/1	36701
15	*R. chalastus*	Hilton Beck, UK	HIL 01	B43/3	36702
16	*R. chalastus*	Conisborough, UK	5031	B47/2	36703
17	*R. chalastus*	Conisborough, UK	5031	F24/4	36704
18	*R. chalastus*	Conisborough, UK	5031	B27	36705

Plate 3

Figure number	Species	Locality	Depth (m)	Slide	England Finder Co-ordinates	CPC Number
1	*R. chalastus*	Dalongkou Anticline (north limb), Junggar, Northern Xinjiang, China	170.5 below top of the Guodikeng Fm.	640 3380 NLD36	D35	36706
2	*R. chalastus*	Dalongkou Anticline (north limb), Junggar, Northern Xinjiang, China	170.5 below top of the Guodikeng Fm.	640 3380 NLD36	P5/1	36707
3	*R. chalastus*	Dalongkou Anticline (north limb), Junggar, Northern Xinjiang, China	170.5 below top of the Guodikeng Fm.	640 3380 NLD36	L35	36708
4	*R. chalastus*	Dalongkou Anticline (north limb), Junggar, Northern Xinjiang, China	170.5 below top of the Guodikeng Fm.	640 3380 NLD36	N21/4	36709
5	*R. chalastus*	Dalongkou Anticline (north limb), Junggar, Northern Xinjiang, China	170.5 below top of the Guodikeng Fm.	640 3380 NLD36 mounted on Stub 7		36710
6	*R. chalastus*	Dalongkou Anticline (north limb), Junggar, Northern Xinjiang, China	170.5 below top of the Guodikeng Fm.	640 3380 NLD36 mounted on Stub 13		36711
7	*R. chalastus*	Dalongkou Anticline (north limb), Junggar, Northern Xinjiang, China	170.5 below top of the Guodikeng Fm.	640 3380 NLD36	N40/2	36712
8	*R. chalastus*	Dalongkou Anticline (north limb), Junggar, Northern Xinjiang, China	170.5 below top of the Guodikeng Fm.	640 3380 NLD36	C20/4	36713
9	*R. chalastus*	Dalongkou Anticline (north limb), Junggar, Northern Xinjiang, China	170.5 below top of the Guodikeng Fm.	640 3380 NLD36	C20/4	36714
10	*R. chalastus*	Dalongkou Anticline (north limb), Junggar, Northern Xinjiang, China	192.5 below top of the Guodikeng Fm.	640 3381 NLD 37	E29/1	36715
11	*R. chalastus*	Dalongkou Anticline (north limb), Junggar, Northern Xinjiang, China	170.5 below top of the Guodikeng Fm.	640 3380 NLD36	P5/1 (detail of Fig.2)	36707
12	*R. chalastus*	Dalongkou Anticline (north limb), Junggar, Northern Xinjiang, China	170.5 below top of the Guodikeng Fm.	640 3380 NLD36	P5/1 (detail of Fig.2)	36707
13	*R. chalastus*	Dalongkou Anticline (north limb), Junggar, Northern Xinjiang, China	170.5 below top of the Guodikeng Fm.	640 3380 NLD36	C12	36716
14	*R. chalastus*	Dalongkou Anticline (north limb), Junggar, Northern Xinjiang, China	170.5 below top of the Guodikeng Fm.	640 3380 NLD36	D17/4	36717
15	*R. chalastus*	Dalongkou Anticline (north limb), Junggar, Northern Xinjiang, China	170.5 below top of the Guodikeng Fm.	640 3380 NLD36	C20/4	36718

Plate 4

Figure number	Species	Locality	Depth (m)	Slide	England Finder Co-ordinates	CPC Number
1	*R. chalastus*	Borehole No. 453K, Shartanovo Village, Vologodskaya Region, Russia	44.4	203.3Russia	T55/1	36719
2	*R. chalastus*	Borehole No. 453K, Shartanovo Village, Vologodskaya Region, Russia	44.4	203.3Russia	D41/4	36720
3	*R. chalastus*	Borehole No. 453K, Shartanovo Village, Vologodskaya Region, Russia	44.4	203.3Russia	L49/2	36721
4	*R. chalastus*	Borehole No. 453K, Shartanovo Village, Vologodskaya Region, Russia	44.4	203.3Russia	F58/1	36722
5	*R. chalastus*	Lutite horizon (Mazzin Member) Tesero Section, Austrian Alps		T1 6403434/2	N31/3	36723
6	*R. chalastus*	Lutite horizon (Mazzin Member) Tesero Section, Austrian Alps		T1 6403434/2	N33/4	36724
7	*R. chalastus*	Lutite horizon (Mazzin Member) Tesero Section, Austrian Alps		T1 6403434/2	N6	36725
8	*R. chalastus*	Lutite horizon (Mazzin Member) Tesero Section, Austrian Alps		T1 6403434/2	O16/3	36726
9	*R. chalastus*	Lutite horizon (Mazzin Member) Tesero Section, Austrian Alps		T1 6403434/2	N8	36727
10	*R. chalastus*	Lutite horizon (Mazzin Member) Tesero Section, Austrian Alps		T1 6403434/2	P15/3	36728
11	*R. chalastus*	Lutite horizon (Mazzin Member) Tesero Section, Austrian Alps		T1 6403434/2 mounted on Stub 1		36729
12	*R. chalastus*	Lutite horizon (Mazzin Member) Tesero Section, Austrian Alps		T1 6403434/2 mounted on Stub 1		36730
13	*R. chalastus*	Lutite horizon (Mazzin Member) Tesero Section, Austrian Alps		T1 6403434/2 mounted on Stub 12		36731
14	*R. chalastus*	Lutite horizon (Mazzin Member) Tesero Section, Austrian Alps		T1 6403434/2 mounted on Stub 12		36732
15	*R. chalastus*	Lutite horizon (Mazzin Member) Tesero Section, Austrian Alps		T1 6403434/2 mounted on Stub 1		36733

Plate 5

Figure number	Species	Locality	Depth (ft)	Slide	England Finder Co-ordinates	CPC Number
1	*R. chalastus*	Borehole DILM-1, central Saudi Arabia	7827.9	DILM-1 7827.9	D31/1	36734
2	*R. chalastus*	Borehole DILM-1, central Saudi Arabia	7827.9	DILM-1 7827.9	N30	36735
3	*R. chalastus*	Borehole DILM-1, central Saudi Arabia	7827.9	DILM-1 7827.9	K49/2	36736
4	*R. chalastus*	Borehole DILM-1, central Saudi Arabia	7827.9	DILM-1 7827.9	Q30/2	36737
5	*R. chalastus*	Borehole DILM-1, central Saudi Arabia	7827.9	DILM-1 7827.9	O45	36738
6	*R. chalastus*	Borehole DILM-1, central Saudi Arabia	7827.9	DILM-1 7827.9	W33	36739
7	*R. chalastus*	Borehole DILM-1, central Saudi Arabia	7827.9	DILM-1 7827.9	C33	36740
8	*R. chalastus*	Borehole DILM-1, central Saudi Arabia	7827.9	DILM-1 7827.9	F43/4	36741
9	*R. chalastus*	Borehole DILM-1, central Saudi Arabia	7827.9	DILM-1 7827.9	K35/1	36742
10	*R. chalastus*	Borehole DILM-1, central Saudi Arabia	7827.9	DILM-1 7827.9	O42/2	36743
11	*R. chalastus*	Borehole DILM-1, central Saudi Arabia	7827.9	DILM-1 7827.9	O45/2	36744
12	*R. chalastus*	Borehole DILM-1, central Saudi Arabia	7827.9	DILM-1 7827.9	O45/2	36745
13	*R. chalastus*	Borehole DILM-1, central Saudi Arabia	7827.9	DILM-1 7827.9 mounted on Stub 6		36746
14	*R. chalastus*	Borehole DILM-1, central Saudi Arabia	7827.9	DILM-1 7827.9 mounted on Stub 6		36747
15	*R. chalastus*	Borehole DILM-1, central Saudi Arabia	7827.9	DILM-1 7827.9 mounted on Stub 6		36748

Plate 6

Figure number	Species	Locality	Slide	England Finder Co-ordinates	CPC Number
1	*R. catenulatus*	Greer County, Oklahoma, USA	Flowerpot WM 2504-1	G41	36749
2	*R. catenulatus*	Greer County, Oklahoma, USA	Flowerpot WM 2504-1	H40/4	36750
3	*R. catenulatus*	Greer County, Oklahoma, USA	Flowerpot WM 2504-1	G44	36751
4	*R. catenulatus*	Greer County, Oklahoma, USA	Flowerpot WM 2504-1	T12/2	36752
5	*R. catenulatus*	Greer County, Oklahoma, USA	Flowerpot WM 2504-1	S33	36753
6	*R. catenulatus*	Greer County, Oklahoma, USA	Flowerpot WM 2504-1	T7/1	36754
7	*R. catenulatus*	Greer County, Oklahoma, USA	Flowerpot WM 2504-1	T22/1	36755
8	*R. catenulatus*	Greer County, Oklahoma, USA	Flowerpot WM 2504-1	S15	36756
9	*R. catenulatus*	Greer County, Oklahoma, USA	Flowerpot WM 2504-1	S35	36757
10	*R. catenulatus*	Greer County, Oklahoma, USA	Flowerpot WM 2504-1	T20	36758
11	*R. catenulatus*	Greer County, Oklahoma, USA	Flowerpot WM 2504-1	E19	36759
12	*R. catenulatus*	Greer County, Oklahoma, USA	Flowerpot WM 2504-1	E19/4	36760
13	*R. catenulatus*	Greer County, Oklahoma, USA	Flowerpot WM 2504-1	E15	36761
14	*R. catenulatus*	Greer County, Oklahoma, USA	Flowerpot WM 2504-1	E19	36762
15	*R. catenulatus*	Greer County, Oklahoma, USA	Flowerpot WM 2504-1	E18	36763
16	*R. catenulatus*	Greer County, Oklahoma, USA	Flowerpot WM 2504-1	N25	36764
17	*R. catenulatus*	Greer County, Oklahoma, USA	Flowerpot WM 2504-1	M39/1	36765
18	*R. catenulatus*	Greer County, Oklahoma, USA	Flowerpot WM 2504-1	T36	36766
19	*R. catenulatus*	Greer County, Oklahoma, USA	Flowerpot WM 2504-1	J27/3	36767
20	*R. catenulatus*	Greer County, Oklahoma, USA	Flowerpot WM 2504-1	N34/4	36768
21	*R. catenulatus*	Greer County, Oklahoma, USA	Flowerpot WM 2504-1	M29/2	36769
22	*R. catenulatus*	Greer County, Oklahoma, USA	Flowerpot WM 2504-1	M24/1	36770
23	*R. catenulatus*	Greer County, Oklahoma, USA	Flowerpot WM 2504-1	E23	36771
24	*R. catenulatus*	Greer County, Oklahoma, USA	Flowerpot WM 2504-1	H10/2	36772
25	*R. catenulatus*	Greer County, Oklahoma, USA	Flowerpot WM 2504-1	E36	36773
26	*R. catenulatus*	Greer County, Oklahoma, USA	Flowerpot WM 2504-1	J11/2	36774
27	*R. catenulatus*	Greer County, Oklahoma, USA	Flowerpot WM 2504-1	J32	36775
28	*R. catenulatus*	Greer County, Oklahoma, USA	Flowerpot WM 2504-1	G36	36776
29	*R. catenulatus*	Greer County, Oklahoma, USA	Flowerpot WM 2504-1	G16	36777
30	*R. catenulatus*	Greer County, Oklahoma, USA	Flowerpot WM 2504-1	G39/2	36778
31	*R. catenulatus*	Greer County, Oklahoma, USA	Flowerpot WM 2504-1	D43	36779
32	*R. catenulatus*	Greer County, Oklahoma, USA	Flowerpot 66398	Y41/4	36775
33	*R. catenulatus*	Greer County, Oklahoma, USA	Flowerpot WM 2504-1	L24/4	36780
34	*R. catenulatus*	Greer County, Oklahoma, USA	Flowerpot WM 2504-1	N23/4	36781
35	*R. catenulatus*	Greer County, Oklahoma, USA	Flowerpot WM 2504-1	L27/4	36782
36	*R. catenulatus*	Greer County, Oklahoma, USA	Flowerpot WM 2504-1	C34	36783

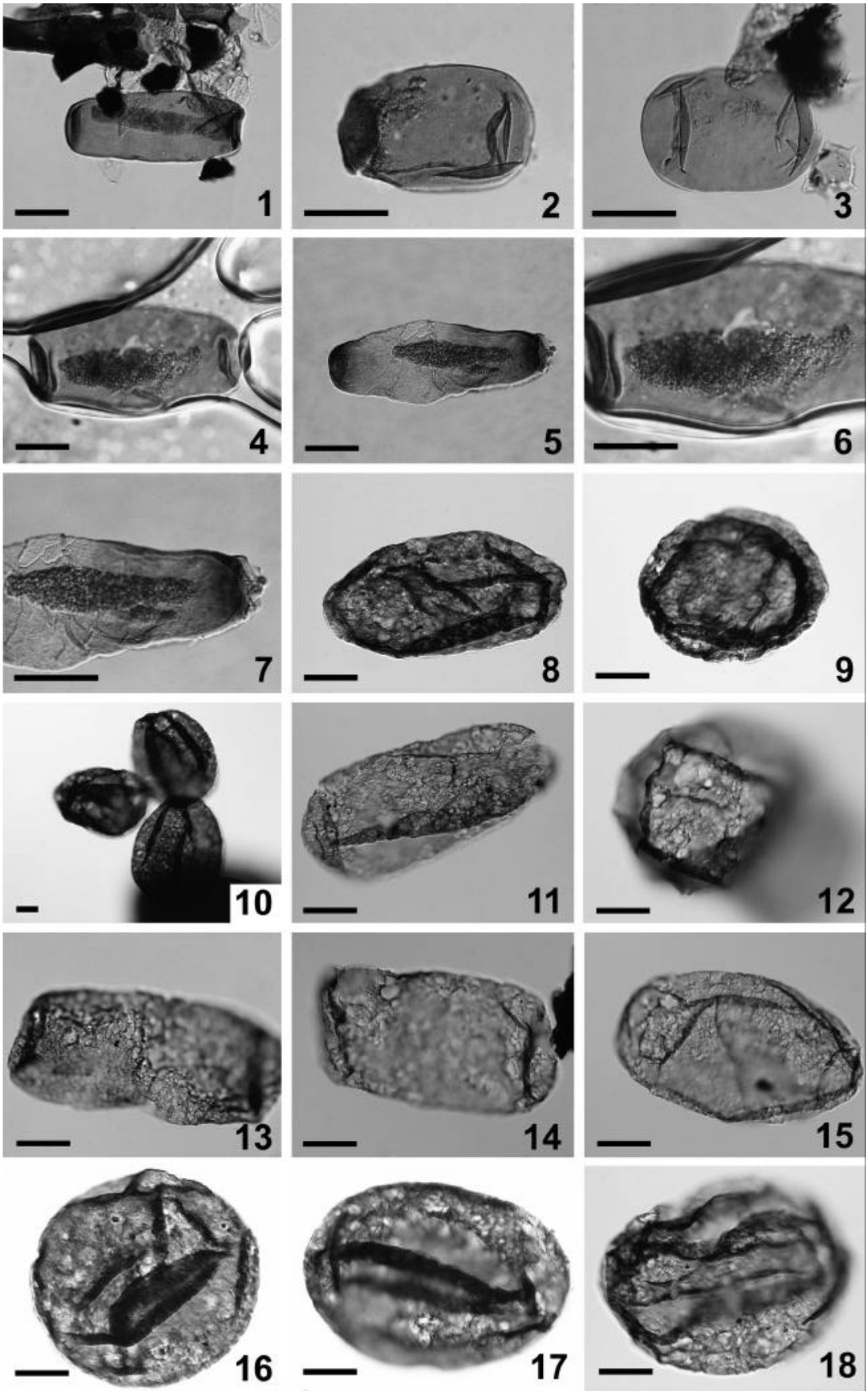
1
2
3
4
5
6
7
8
9
10
11
12
13
14
15
16
17
18

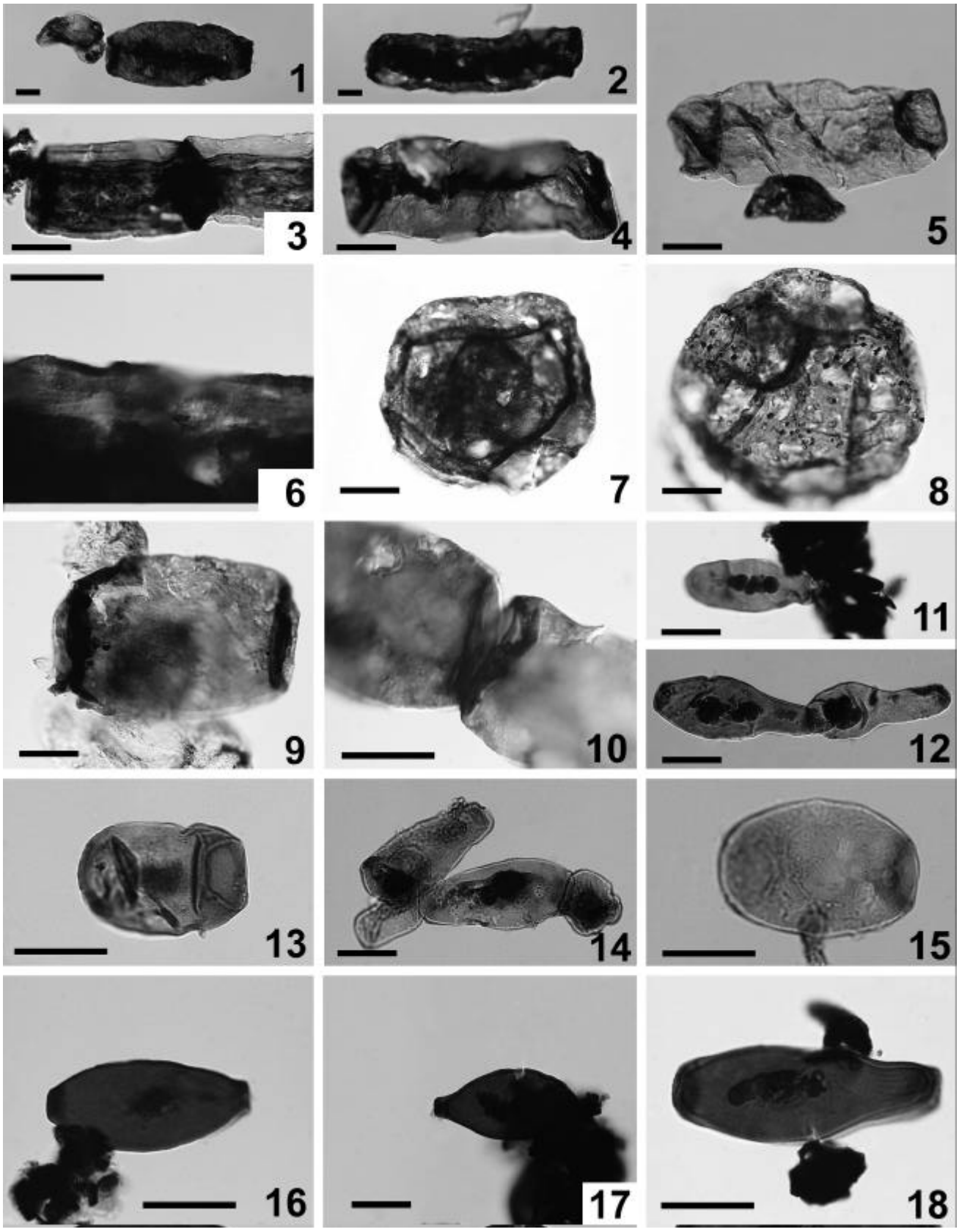
1
2
3
4
5
6
7
8
9
10
11
12
13
14
15
16
17
18

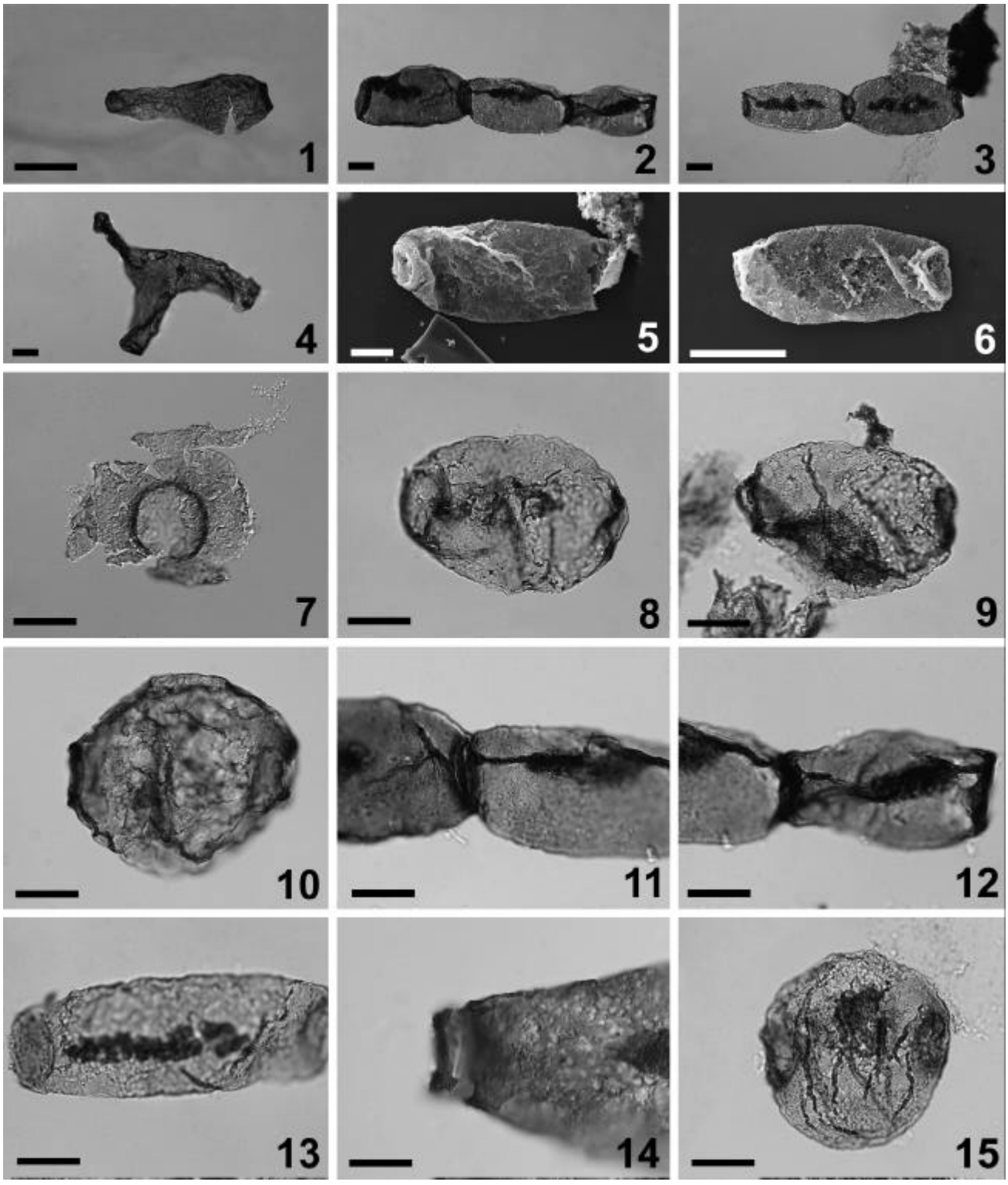
1
2
3
4
5
6
7
8
9
10
11
12
13
14
15

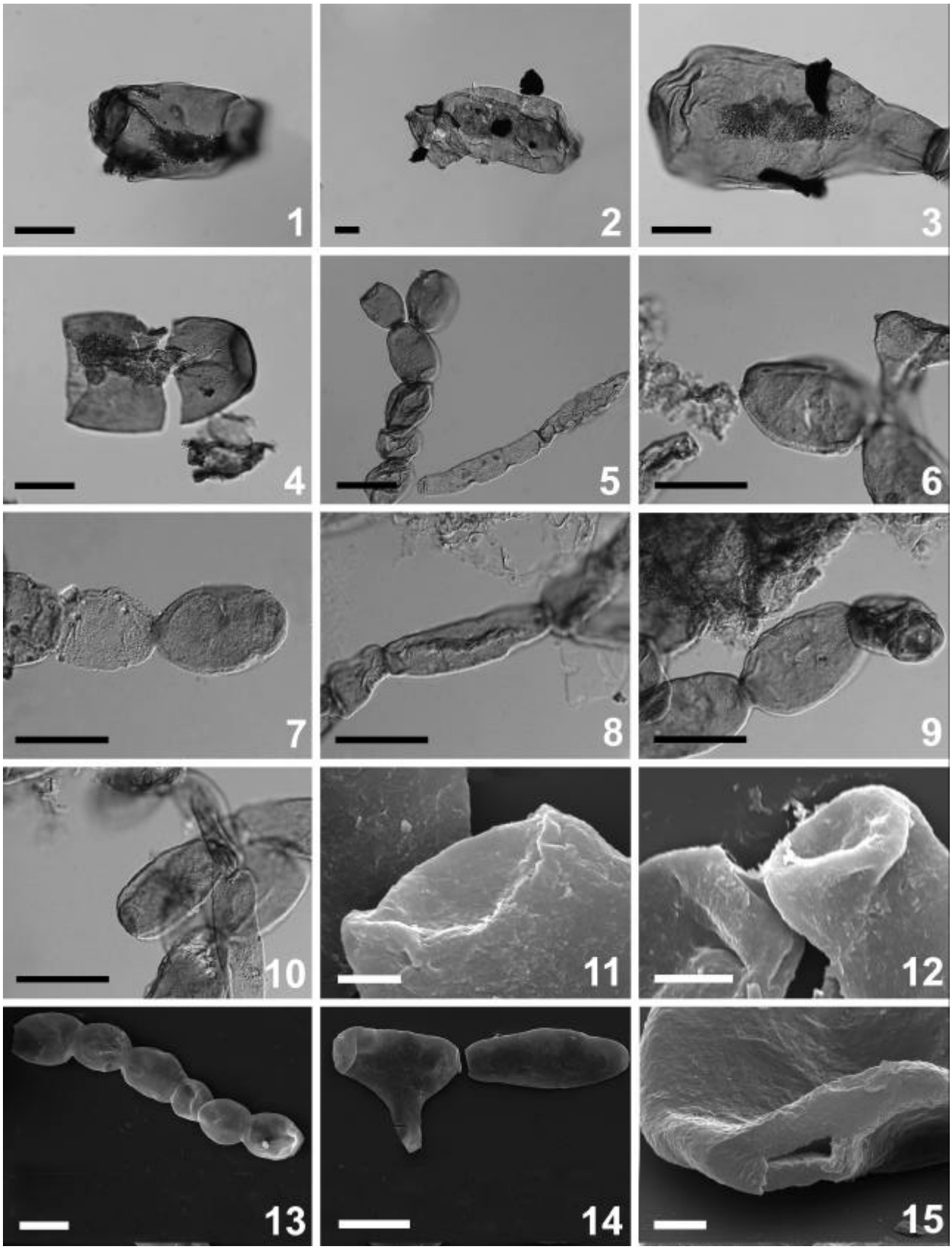
1
2
3
4
5
6
7
8
9
10
11
12
13
14
15

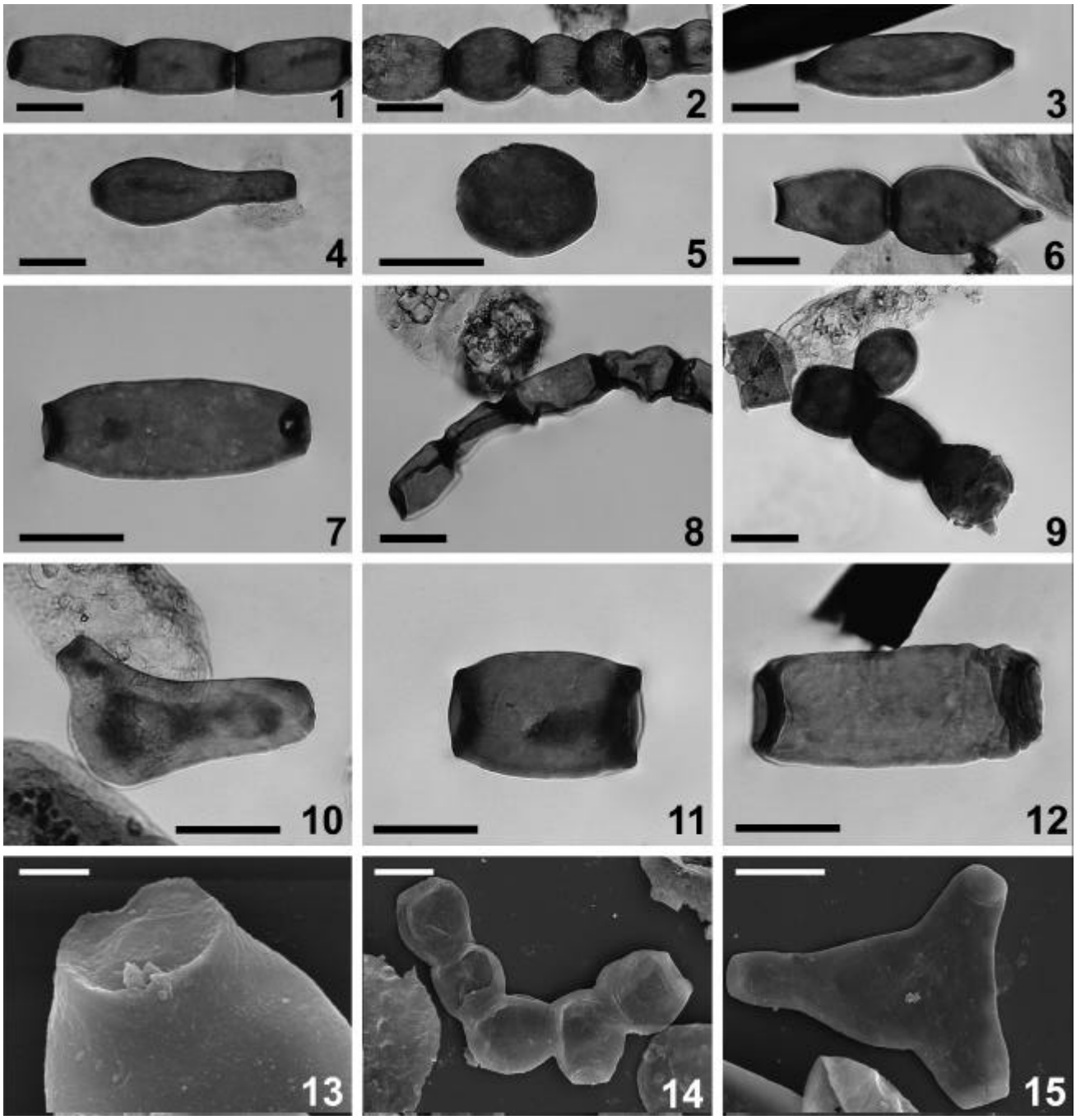
1
2
3
4
5
6
7
8
9
10
11
12
13
14
15

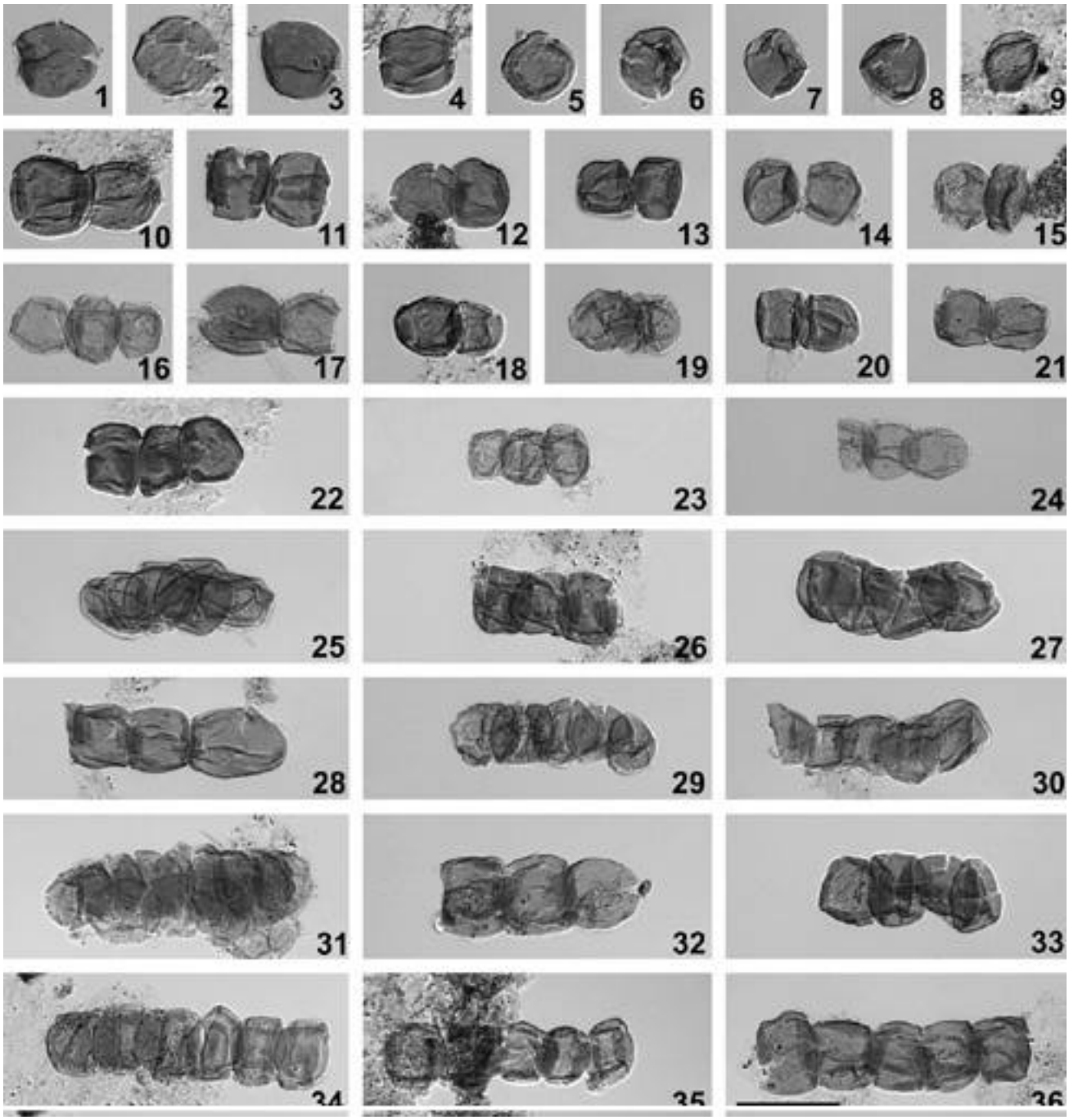
1
2
3
4
5
6
7
8
9
10
11
12
13
14
15
16
17
18
19
20
21
22
23
24
25
26
27
28
29
30
31
32
33
34
35
36

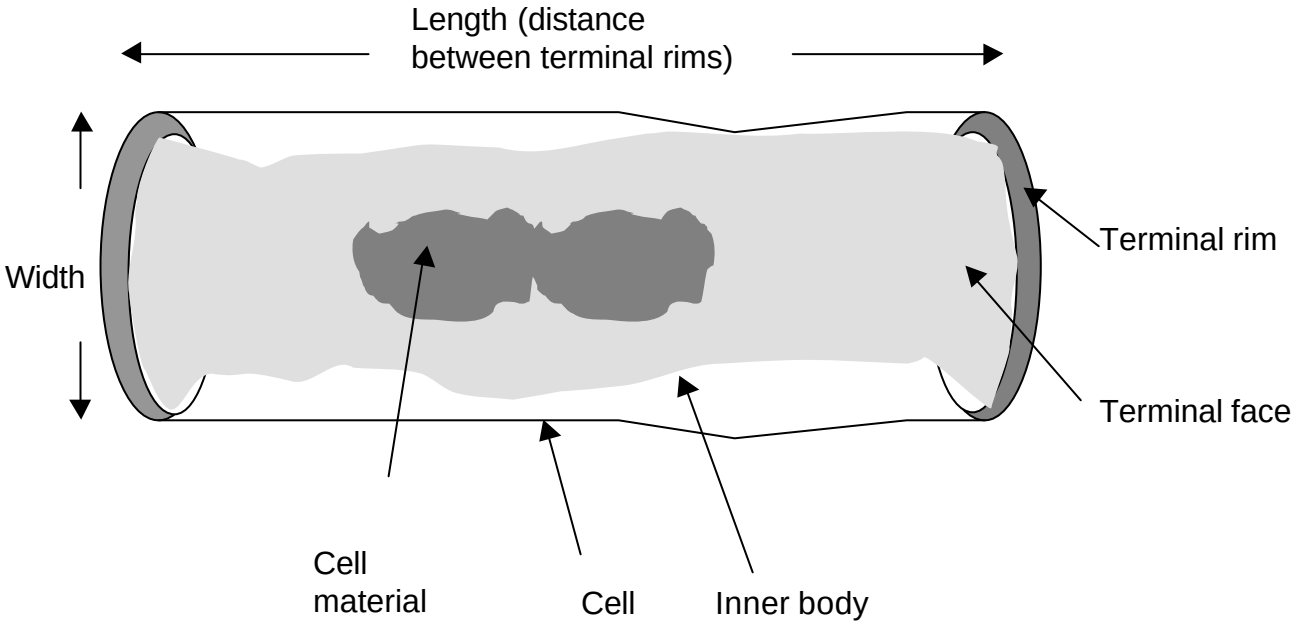
Length (distance
between terminal rims)
Width
Terminal rim
Terminal face
Cell
material
Cell
Inner body

Text Fig 2

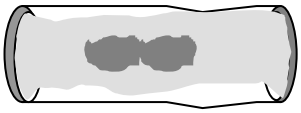

(1)

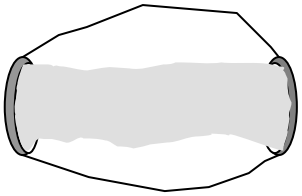

(2)

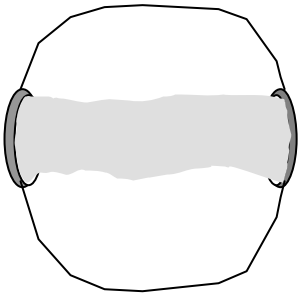

(3)

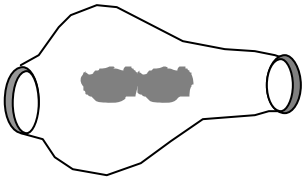

(4)

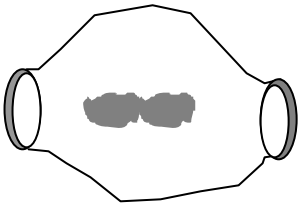

(5)

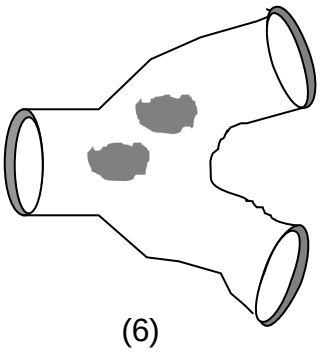

(6)

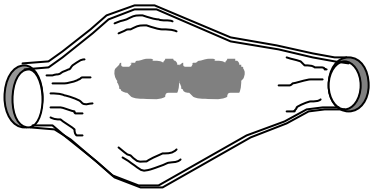

(7)

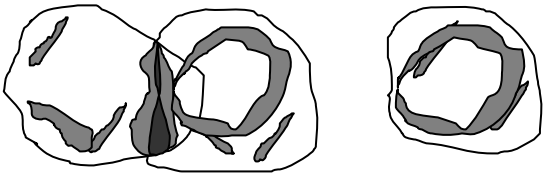

(8)

Fig. 3

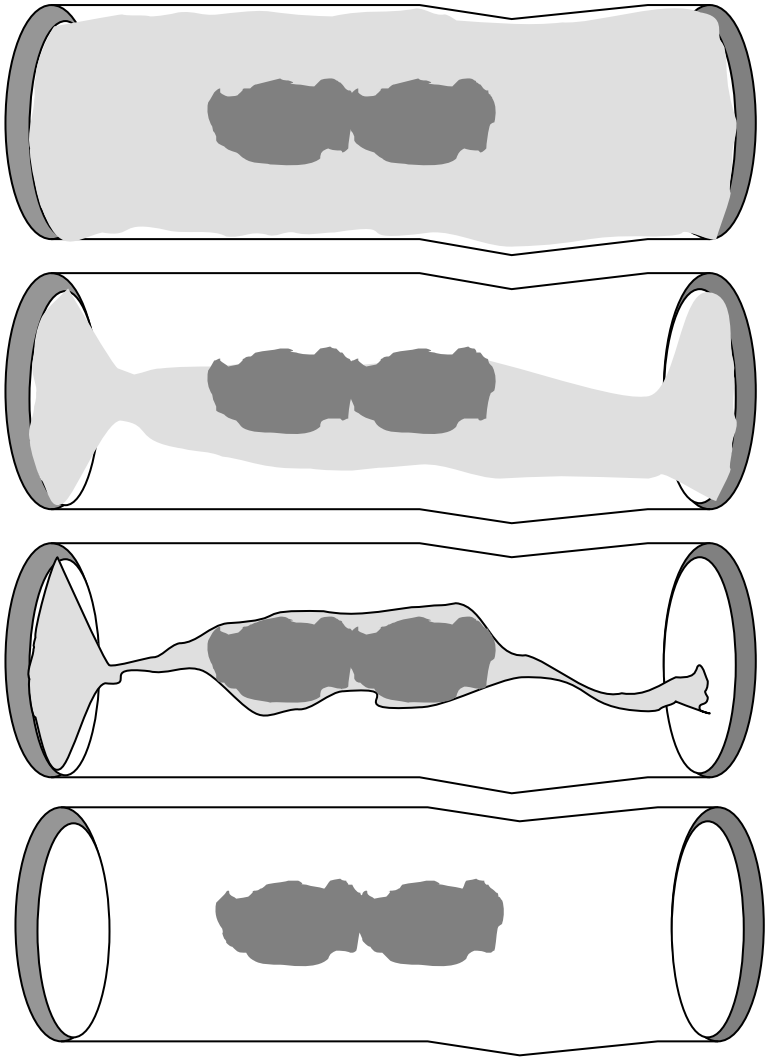

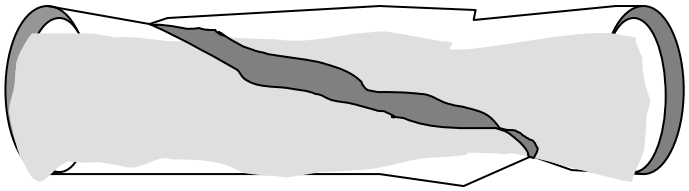

1

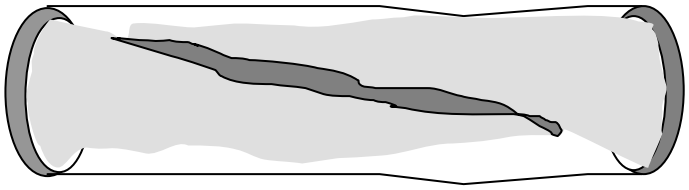

2

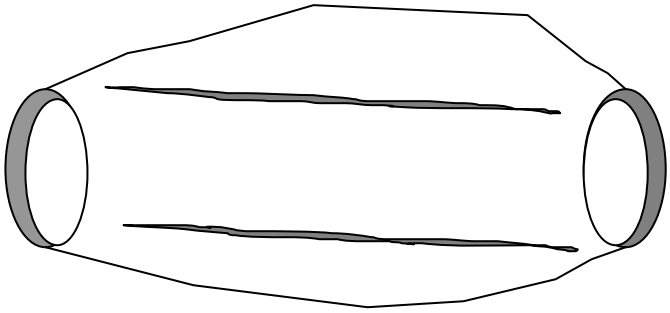

3

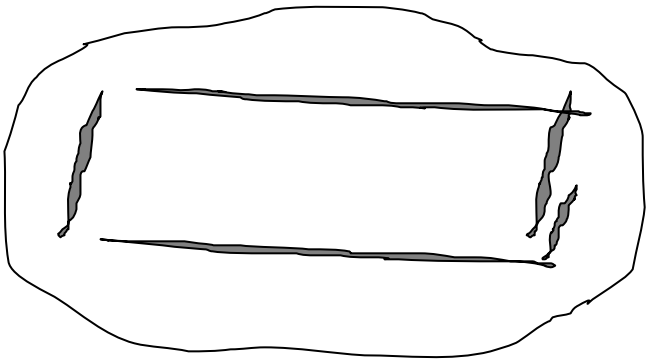

4

Fig. 4

Fig 5

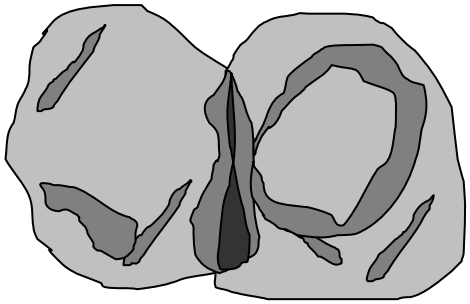

1

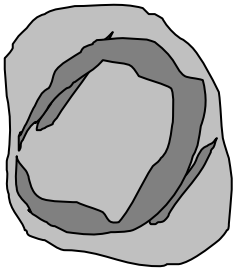

2

Fig. 6

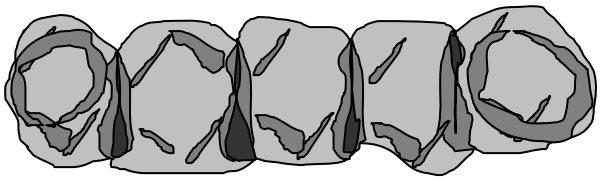

1

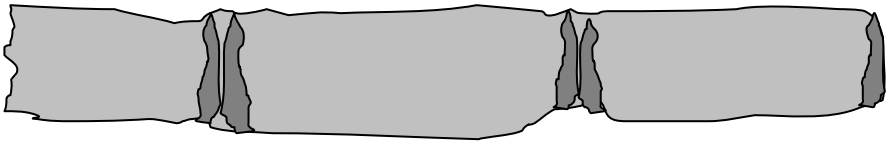

2

Fig. 7

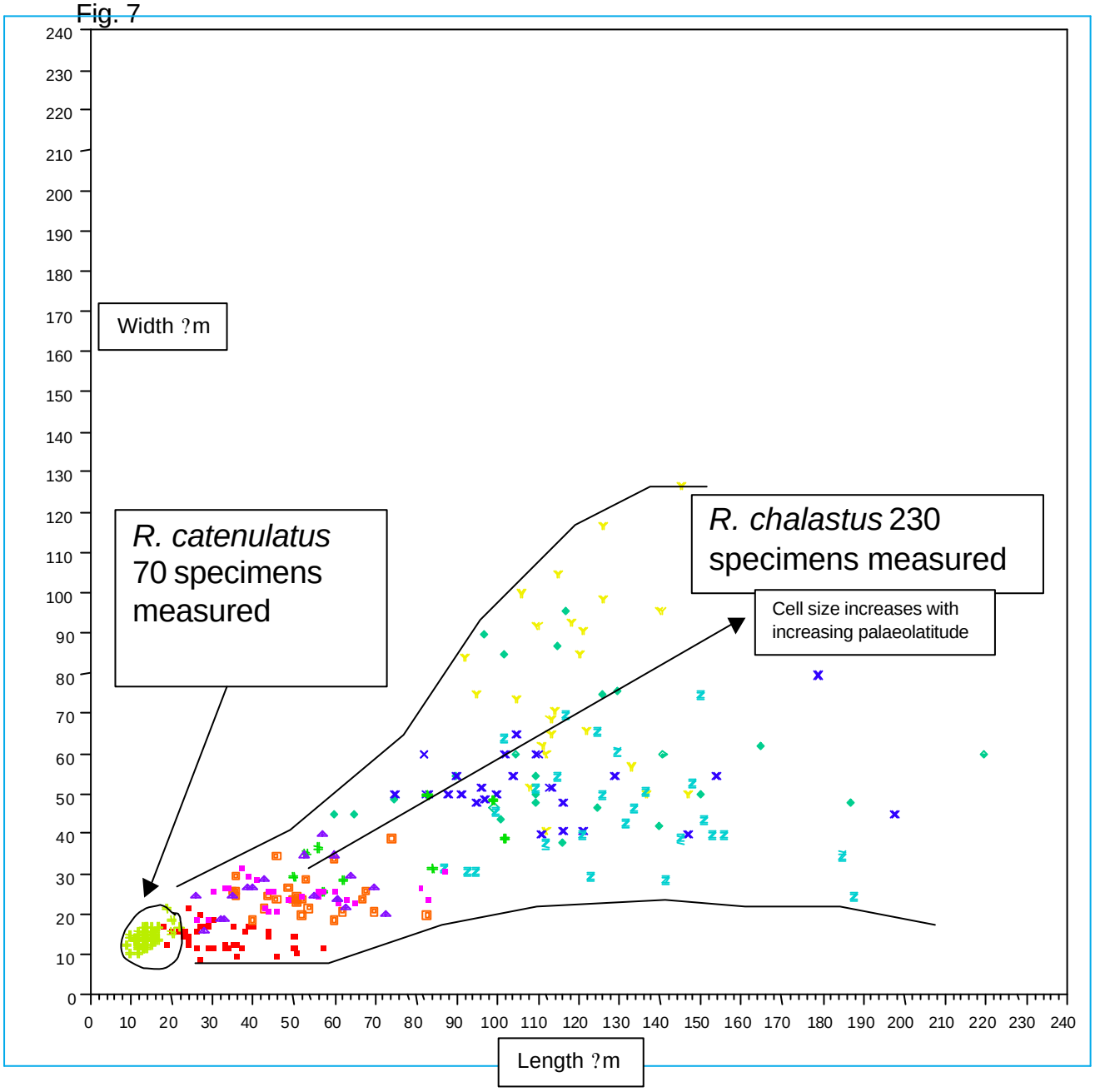
Width ?m
R. catenulatus 70 specimens measured
R. chalastus 230 specimens measured
Cell size increases with increasing palaeolatitude
Length ?m
0
10
20
30
40
50
60
70
80
90
100
110
120
130
140
150
160
170
180
190
200
210
220
230
240

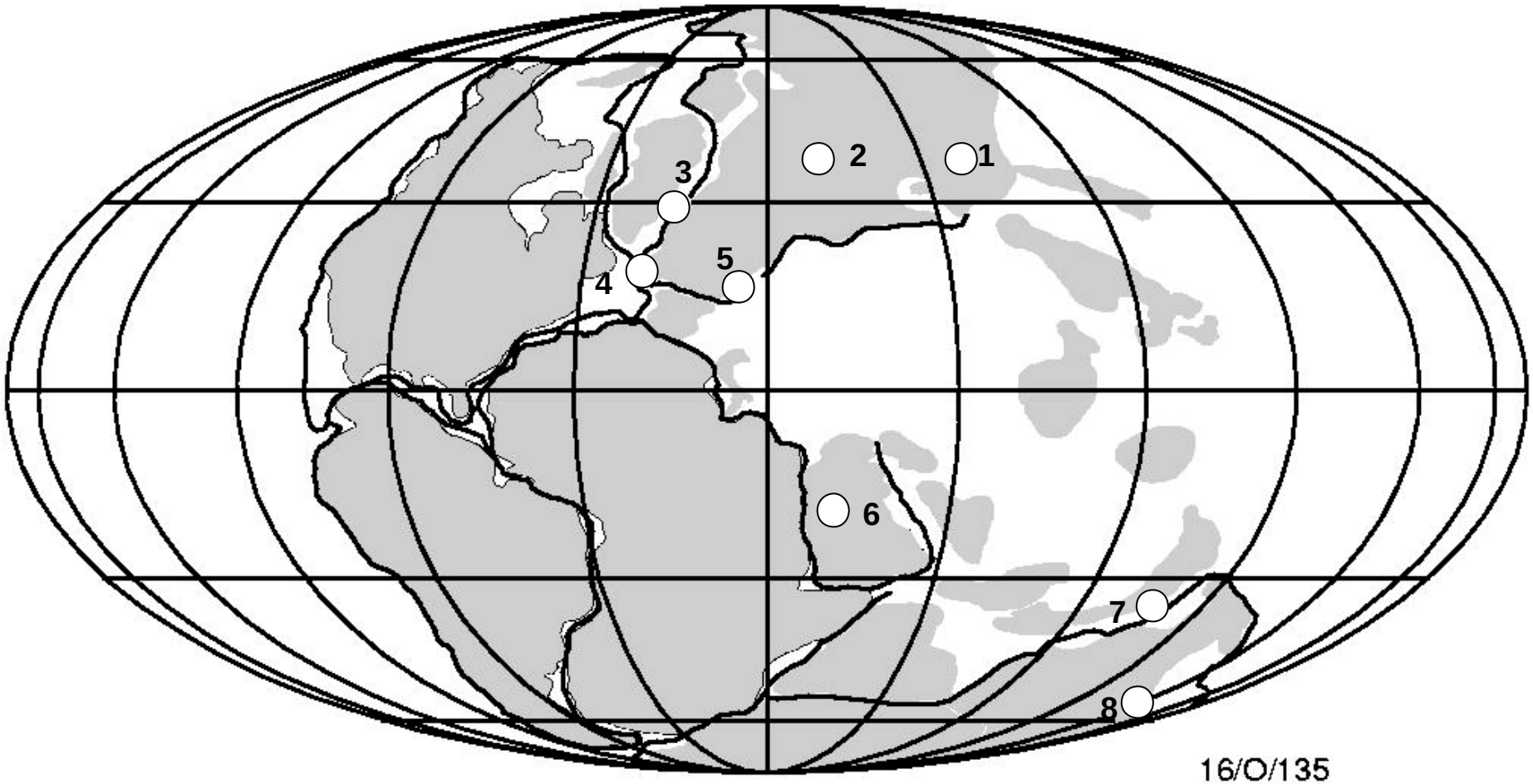
1
2
3
4
5
6
7
8
16/O/135

Fig. 9

			This study										Other records											
Location (all records for *R. chalastus* except for # for *R. catenulatus*)			Greenland	Moura, Australia	Billawock, Australia	Junggar, Northern Xinjiang, China	Russia, Vologodskaya	DILM-1 well, Saudi Arabia	Tesero Austria	Hilton Plant Beds, UK	Conisborough, UK	Greer County ,Oklahoma, USA #	Transdanubia, Hungary (Broglio Loriga et al. 1990)	Sverdrup Basin, Canadian Arctic (Utting 1994)	Barents Sea (Mangerud 1994)	East Africa (Hankel 1992)	Malagasy (Wright & Askin 1987)	Israel (Eshet et al. 1995)	Iraq, Late Permian (Nader et al. 1993)	Greenland (Utting & Piasecki 1995)	Meishan, China (Ouyang & Utting 1990)	Tunisia (Kilani-Mazraoui et al. 1990)	Spitsbergen, Svalvbard (Mangerud & Konieczny 1993)	Russia Lozovsky & Esaulova (1998)
Standard scale	**Tethys scale**	**Traditional standard**																						
Griesbach.			*			*	*		*				*	*	*	*	*	*						*
Changhs.	Dorshamian	Tatarian		*	*	*		*	*	*	*					*		*	*		*	?	*	*
Wuchiaping.	Dzhulfian									*	*									*				
Capitanian	Midian																			*				
Wordian	Murgabian	Kazanian										*												
Roadian	Kubergand.	Ufimian										?												

Fig 10

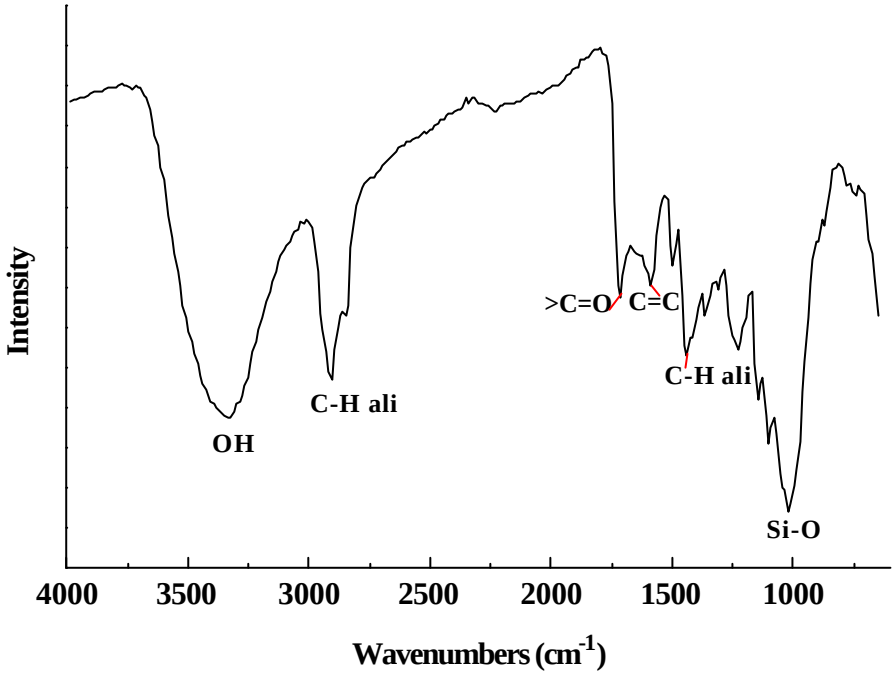
Intensity
OH
C-H ali
>C=O
C=C
C-H ali
Si-O
4000
3500
3000
2500
2000
1500
1000
Wavenumbers (cm-1)

Fig 11

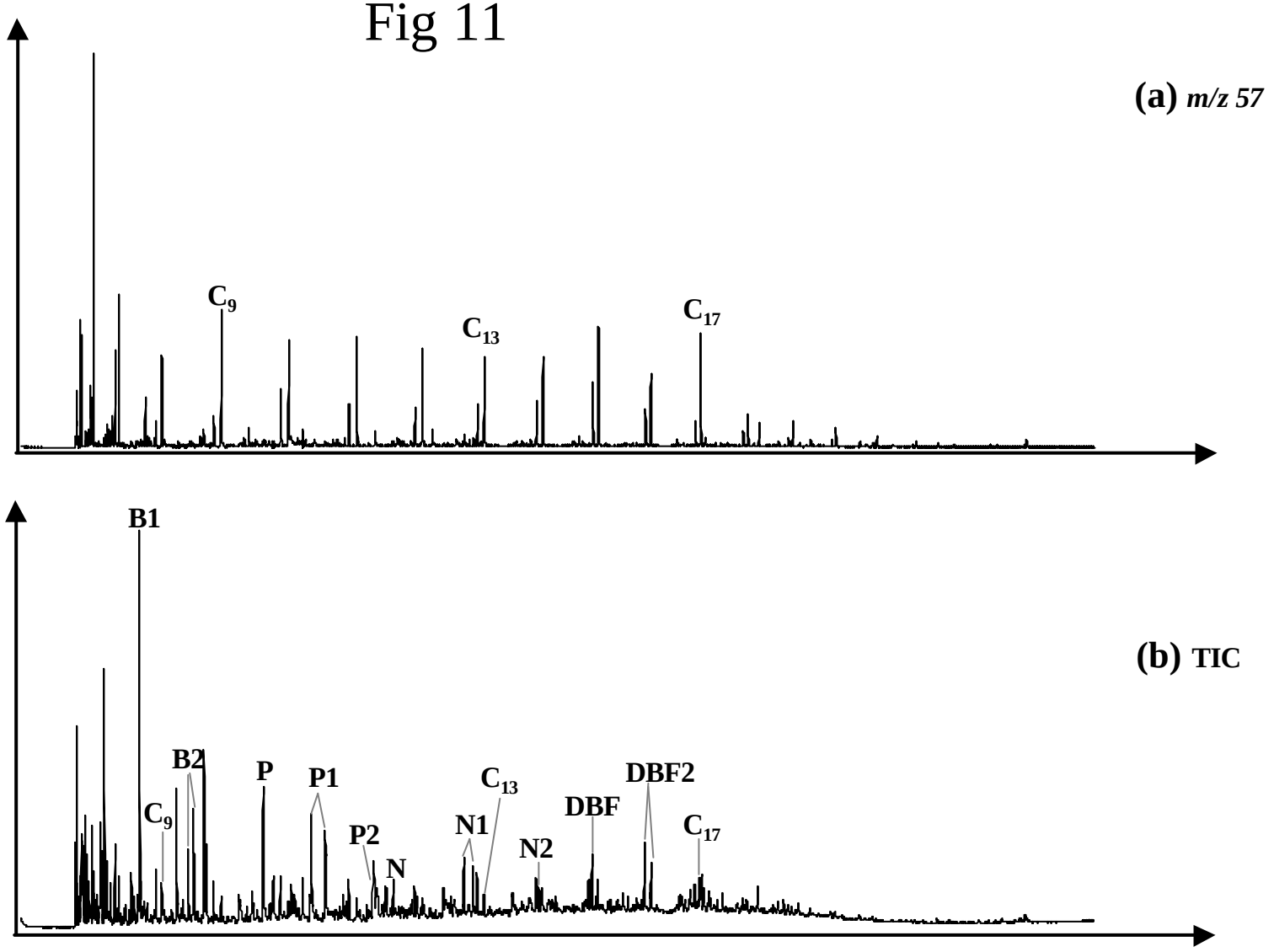
(a) m/z 57
C9
C13
C17
B1
B2
P
P1
P2
N
N1
C13
N2
DBF
DBF2
C17
C9
(b) TIC
Retention Time